The ATLAS[3D] project – VIII. Modelling the formation and evolution of fast and slow rotator early-type galaxies within ΛCDM

Sadegh Khochfar,[1][*] Eric Emsellem,[2,3] Paolo Serra,[4] Maxime Bois,[2,3] Katherine Alatalo,[5] R. Bacon,[3] Leo Blitz,[5] Frédéric Bournaud,[6] M. Bureau,[7] Michele Cappellari,[7] Roger L. Davies,[7] Timothy A. Davis,[7] P. T. de Zeeuw,[2,8] Pierre-Alain Duc,[9] Davor Krajnović,[2] Harald Kuntschner,[10] Pierre-Yves Lablanche,[3] Richard M. McDermid,[11] Raffaella Morganti,[4,12] Thorsten Naab,[13] Tom Oosterloo,[4,6] Marc Sarzi,[14] Nicholas Scott,[7] Anne-Marie Weijmans[15][†] and Lisa M. Young[16]

[1]*Max-Planck Institut für extraterrestrische Physik, PO Box 1312, D-85478 Garching, Germany*
[2]*European Southern Observatory, Karl-Schwarzschild-Str. 2, 85748 Garching, Germany*
[3]*Université Lyon 1, Observatoire de Lyon, Centre de Recherche Astrophysique de Lyon and Ecole Normale Supérieure de Lyon, 9 avenue Charles André, F-69230 Saint-Genis Laval, France*
[4]*Netherlands Institute for Radio Astronomy (ASTRON), Postbus 2, 7990 AA Dwingeloo, the Netherlands*
[5]*Department of Astronomy, Campbell Hall, University of California, Berkeley, CA 94720, USA*
[6]*Laboratoire AIM Paris-Saclay, CEA/IRFU/SAp CNRS Université Paris Diderot, 91191 Gif-sur-Yvette Cedex, France*
[7]*Sub-department of Astrophysics, University of Oxford, Denys Wilkinson Building, Keble Road, Oxford OX1 3RH*
[8]*Sterrewacht Leiden, Leiden University, Postbus 9513, 2300 RA Leiden, the Netherlands*
[9]*Laboratoire AIM, CEA/DSM-CNRS-Universit Paris Diderot, Dapnia/Service d'Astrophysique, CEA-Saclay, 91191 Gif-sur-Yvette Cedex, France*
[10]*Space Telescope European Coordinating Facility, European Southern Observatory, Karl-Schwarzschild-Str. 2, 85748 Garching, Germany*
[11]*Gemini Observatory, Northern Operations Centre, 670 N. A'ohoku Place, Hilo, HI 96720, USA*
[12]*Kapteyn Astronomical Institute, University of Groningen, Postbus 800, 9700 AV Groningen, the Netherlands*
[13]*Max-Planck Institut für Astrophysik, Karl-Schwarzschild-Str. 1, 85741 Garching, Germany*
[14]*Centre for Astrophysics Research, University of Hertfordshire, Hatfield, Herts AL1 9AB*
[15]*Dunlap Institute for Astronomy & Astrophysics, University of Toronto, 50 St George Street, Toronto, ON M5S 3H4, Canada*
[16]*Department of Physics, New Mexico Institute of Mining and Technology, Socorro, NM 87801, USA*

ABSTRACT

We propose a simple model for the origin of fast and slow rotator early-type galaxies (ETG) within the hierarchical Λcold dark matter (ΛCDM) scenario, that is based on the assumption that the mass fraction of stellar discs in ETGs is a proxy for the specific angular momentum expressed via λ_R. Within our model we reproduce the fraction of fast and slow rotators as a function of magnitude in the ATLAS[3D] survey, assuming that fast-rotating ETGs have at least 10 per cent of their total stellar mass in a disc component. In agreement with ATLAS[3D] observations we find that slow rotators are predominantly galaxies with $M_* > 10^{10.5}\,\mathrm{M}_{\odot}$ contributing ∼20 per cent to the overall ETG population. We show in detail that the growth histories of fast and slow rotators are different, supporting the classification of ETGs into these two categories. Slow rotators accrete between ∼50 and 90 per cent of their stellar mass from satellites and their most massive progenitors have on average up to three major mergers during their evolution. Fast rotators in contrast accrete less than 50 per cent and have on average less than one major merger in their past.

We find that the underlying physical reason for the different growth histories is the slowing down and ultimately complete shut-down of gas cooling in massive galaxies. Once cooling and associated star formation in disc stop, galaxies grow via infall from satellites. Frequent minor

[*]E-mail: sadeghk@mpe.mpg.de
[†]Dunlap Fellow.

mergers thereby destroy existing stellar discs via violent relaxation and also tend to lower the specific angular momentum of the main stellar body, lowering λ_R into the slow rotator regime.

On average, the last gas-rich major merger interaction in slow rotators happens at $z > 1.5$, followed by a series of minor mergers. These results support the idea that kinematically decoupled cores (KDC) form during gas-rich major mergers at high z followed by minor mergers, which build-up the outer layers of the remnant, and make remnants that are initially too flat compared to observations become rounder. Fast rotators are less likely to form such KDCs due to the fact that they have on average less than one major merger in their past.

Fast rotators in our model have different formation paths. The majority, 78 per cent, has bulge-to-total stellar mass ratios $(B/T) > 0.5$ and managed to grow stellar discs due to continued gas cooling or bulges due to frequent minor mergers. The remaining 22 per cent live in high-density environments and consist of low B/T galaxies with gas fractions below 15 per cent, that have exhausted their cold gas reservoir and have no hot halo from which gas can cool. These fast rotators most likely resemble the flattened disc-like fast rotators in the ATLAS[3D] survey.

Our results predict that ETGs can change their state from fast to slow rotator and vice versa, while the former is taking place predominantly at low z $(z < 2)$, the latter is occurring during cosmic epochs when cooling times are short and galaxies gas-rich. We predict that the ratio of the number density of slow to fast rotators is a strong function of redshift, with massive $(>10^{10} \, \mathrm{M_\odot})$ fast rotators being more than one order of magnitude more frequent at $z \sim 2$.

1 INTRODUCTION

Much attention has been paid to the modelling of the formation of early-type galaxies (ETGs) over the last three decades (e.g. Toomre & Toomre 1972; White 1978; Negroponte & White 1983; Barnes & Hernquist 1992; Mihos & Hernquist 1996; Naab & Burkert 2003; Bournaud, Combes & Jog 2004; Cox et al. 2006; Hoffman et al. 2010). Once believed to be coeval featureless stellar systems in virial equilibrium that formed from a 'monolithic' collapse (Larson 1974), ever-increasing wealth of observational data have revealed a multitude of distinct physical properties: in their rotational support (Binney 1978; Davies et al. 1983), isophotal shape (Bender et al. 1989; Kormendy & Bender 1996), photometric profiles (Ferrarese et al. 1994; Lauer et al. 1995; Kormendy et al. 2009) and in their stellar angular momentum (Emsellem et al. 2007; Cappellari et al. 2007). Driven by such observations theoretical models have been put to the test, and in particular the Λcold dark matter (ΛCDM) paradigm for structure formation itself within which structure grows hierarchically via a sequence of mergers and accretion events (White & Rees 1978).

Early numerical N-body simulations (Toomre & Toomre 1972) identified galaxy mergers as a viable mechanism to transform dynamical cold stellar systems into dynamical hot ones resembling ETGs with a de Vaucouleurs-like light profile (see also Barnes & Hernquist 1992; Naab & Trujillo 2006). The main driver for this morphological transformation being violent relaxation (Lynden-Bell 1967) during which stars get redistributed. The merger scenario subsequently has been tested against two main categories of observational data: global properties in large homogenous surveys (e.g. Bernardi et al. 2003) and detailed high-resolution observations of an inhomogeneous set of individual galaxies (e.g. de Zeeuw et al. 2002).

Galaxy formation models, in particular semi-analytic models, employing the merger scenario, successfully reproduce the mass function, colour distribution, star formation history and metallicity of ETGs as observed e.g. in the Sloan Digital Sky Survey (SDSS) (e.g. De Lucia et al. 2006). However, they still have problems in e.g. recovering the trend in α/Fe with stellar velocity dispersion (Thomas et al. 2005; Nagashima et al. 2005) or the joint distribution in sizes and velocity dispersion at $z = 0$ (van der Wel et al. 2009; Shankar et al. 2010). The latter has also been reflected in mismatches to the Fundamental Plane of ETGs (Almeida, Baugh & Lacey 2007). While the deviations regarding the sizes and velocity dispersions likely stem from too efficient in-situ star formation in progenitors of present-day ETGs (Shankar et al. 2010), the failure to produce enough α-elements is most likely connected to a combination of too much residual star formation (Thomas et al. 2005) and satellite infall (Khochfar & Silk 2006a).

The inner parts of early-types show further detailed characteristics in the form of steep increasing power law or core-like profiles (Ferrarese et al. 1994; Lauer et al. 1995; Kormendy et al. 2009). The former has been associated with cold gas in discs that loses its angular momentum during the merging process (e.g. Barnes & Hernquist 1991) and settles to the centre of the remnant where it triggers a starburst, thereby steepening the light profile (Hopkins et al. 2008). Core galaxies on the other hand are most likely the product of a *non-dissipative* merger event between two galaxies hosting super-massive black holes (SMBH) at their centre (Milosavljević & Merritt 2001; Khochfar & Burkert 2005; Hopkins et al. 2009c). During the inwards spiralling the SMBH pair kick out stars via three-body interaction and produce a density core in the centre of the remnant (Milosavljević & Merritt 2001).

Classifying elliptical galaxies by the deviation of their isophotal shape from pure ellipses has been suggested as a method to separate the population of elliptical galaxies into two classes with box-like (boxy) and disc-like deviations (discy) (Bender et al. 1989). Numerical simulations show that equal-mass mergers in general produce remnants with boxy isophotes due to stronger gravitational interaction and associated violent relaxation (Bendo & Barnes 2000; Naab & Burkert 2003) efficiently destroying progenitor discs. In contrast

unequal mass major mergers with $2 \leq M_1/M_2 \leq 4$ result on average in discy remnants for the majority of projections under which they are viewed (Naab & Burkert 2003). Observationally, the average isophotal shape of elliptical galaxies turns towards boxy going up in mass (see however Emsellem et al. 2011, hereafter Paper III) indicating a transition in the formation process of massive ellipticals that cannot be attributed to the mass ratio during the last major merger alone, which in general does not change significantly enough in frequency as a function of mass (Khochfar & Burkert 2005). In addition unequal-mass mergers of ETGs are able to transform discy ellipticals into boxy ones in the majority of simulated cases (Naab, Khochfar & Burkert 2006). Within a cosmological context the relative fraction of dry, early-type major mergers increases with stellar mass of the remnant (Khochfar & Burkert 2003) providing the additional channel needed to recover the observed trend with mass (Khochfar & Burkert 2005). In a detailed study of the orbital content of stars in merger remnants, Jesseit, Naab & Burkert (2005) showed that the individual mixture of orbits is the deciding factor on the isophotal shape of discy and boxy elliptical galaxies.

Making full use of the dynamical information available in integral-field observations the SAURON sample (de Zeeuw et al. 2002) measured the specific baryonic angular momentum content via the proxy λ_R within one R_e of a representative sample of ETGs and separate them into fast and slow rotators according to their λ_R value, in a robust way that is nearly insensitive to projection effects (Cappellari et al. 2007; Emsellem et al. 2007). Observationally, fast rotators present regular rotation patterns aligned with the photometry, while slow rotators have low angular momentum content and show misalignments between the photometry and the velocity axes and often exhibit kinematically distinct cores (KDC; Krajnović et al. 2008). The division into fast and slow rotators is further supported by recent simulations of Bois et al. (2011, hereafter Paper VI) that show that fast (respectively slow) rotators have a high (respectively low) angular momentum content, their photometric and kinematic position angle are aligned (respectively misaligned) and they present (respectively do not present) regular velocity patterns. While the SAURON survey was biased towards massive ETGs (de Zeeuw et al. 2002) the ATLAS[3D] survey (Cappellari et al. 2011a, hereafter Paper I) for the first time allows us to give a complete view of the local ETG population within a radius of 42 Mpc using the full information of integral-field observations. The combination of completeness with detailed structural information and complementary observations on e.g. the H I (Serra et al., in preparation) or molecular (Young et al. 2011, hereafter Paper IV) gas masses make the ATLAS[3D] survey an ideal data set to investigate the formation of ETGs.

In this paper we attempt to model fast and slow rotators within the standard ΛCDM paradigm and analyse specific differences in their formation. The structure of the paper is as follows: we start by summarizing the basic model ingredients used in our semi-analytic modelling (SAM) approach in Section 2, followed by showing the performance of the model in Section 3. In Section 4 we introduce our model for fast and slow rotators and investigate the robustness of our assumptions before we analyse in detail differences in their formation in Section 5 and predict their redshift evolution in Section 6. Section 7 is devoted to the question of cosmic variance in the ATLAS[3D] sample followed by Sections 8 and 9 in which we summarize our results and conclude, respectively.

2 THE MODELLING APPROACH

We apply the SAM approach to galaxy formation pioneered in a series of papers (e.g. Rees & Ostriker 1977; Silk 1977; White &

Rees 1978; White & Frenk 1991). The main strategy behind SAMs is to first calculate the collapse and merging history of individual dark matter haloes, and secondly to approximate the more complex physics of the baryons inside these dark matter haloes by analytic models (see e.g. Somerville & Primack 1999; Cole et al. 2000; Hatton et al. 2003; Cattaneo et al. 2006; Croton et al. 2006; Bower et al. 2006; Kang, Jing & Silk 2006; De Lucia & Blaizot 2007; Khochfar & Silk 2009b; Kauffmann et al. 1999, hereafter K99). Each of the dark matter haloes will consist of three main components which are distributed among individual galaxies inside them: a stellar, a cold and a hot gas component, where the latter is only attributed to *central* galaxies, which are the most massive galaxies inside individual haloes and are typically observed to reside in extended X-ray emitting hot haloes of gas (Mulchaey & Jeltema 2010). In the following sections, we will describe briefly the recipes used to calculate these different components which are mainly based on recipes presented in e.g. K99 and Springel et al. (2001) (hereafter S01), and we refer readers for more details on the basic model implementations to their work and references therein. In the remainder of this paper we call SAM the model implementation presented in Khochfar & Burkert (2003, 2005) which is summarized in the following parts of this section. With our SAM we model a cosmic volume of $V_{A3D} = 10^5$ Mpc^3, which is comparable to the volume of the ATLAS[3D] survey (Paper I). Throughout this paper, we use the following set of cosmological parameters consistent with 7-year *Wilkinson Microwave Anisotropy Probe* data (Komatsu et al. 2011): $\Omega_0 = 0.26$, $\Omega_\Lambda = 0.74$, $\Omega_b/\Omega_0 = 0.17$, $n_s = 0.97$, $\sigma_8 = 0.8$ and $h = 0.71$.

2.1 Dark matter

The mass function of dark matter haloes within our volume is calculated using the analytic fitting formula of Jenkins et al. (2001). In addition, to investigate the effects of cosmic variance (see Section 7) we have run a cosmological *N*-body simulation of a $(100 \, \text{Mpc} \, h^{-1})^3$ volume with GADGET-2 (Springel 2005). The particle resolution of the simulation is $10^9 \, \text{M}_\odot \, h^{-1}$, and we generate the $z = 0$ halo mass function using the friends-of-friends (FOF) algorithm.

The corresponding halo merging histories are calculated using a Monte Carlo approach based on the Extended Press–Schechter formalism (e.g. Lacey & Cole 1993) following the method presented in Somerville & Kolatt (1999). This approach has been shown to produce merging histories and progenitor distributions in reasonable agreement with results from *N*-body simulations of CDM structure formation in a cosmological context (Somerville et al. 2000). The merging history of dark matter haloes is reconstructed by breaking each halo up into progenitors above a limiting minimum progenitor mass M_{min}. This mass cut needs to be chosen carefully as it ensures that the right galaxy population and merging histories are produced within the model. Progenitor haloes with masses below M_{min} are declared as *accretion* events and their histories are not followed further back in time. Progenitors labelled as accretion events should ideally not host any significant galaxies in them and be composed mainly of primordial gas. To achieve a good compromise between accuracy and computational time, we estimate M_{min} by running several simulations with different resolutions and chose the resolution for which results in the galaxy mass range of interest are independent of the specific choice of M_{min}. Changing the mass resolution mainly affects our results at low galaxy mass scales, leaving massive galaxies, the focus of this work, literally unaffected. Throughout this paper we will use $M_{min} = 10^{10} \, \text{M}_\odot$ which produces numerically stable results for galaxies with stellar masses greater than $\sim 6 \times 10^9 \, \text{M}_\odot$,

which corresponds to the mass limit in the ATLAS[3D] survey. For simplicity, we assume in the following that the dark matter profiles are that of truncated isothermal spheres (K99).

2.2 Baryonic physics

Once the merging history of the dark matter component has been calculated, it is possible to follow the evolution of the baryonic content in these haloes forward in time. We assume each halo consists of three components: hot gas (M_{hot}), cold gas (M_{gas}) and stars (M_*), where the latter two components can be distributed among individual galaxies, labelled *central* and *satellite*, inside a single dark matter halo. The hot gas component, however, is only associated with central galaxies. The stellar component of each galaxy is additionally divided into bulge (M_{bul}) and disc (M_{disc}) to allow the morphological classification of model galaxies. In the following, we describe how the evolution of each component is calculated.

2.2.1 Gas cooling and reionization

Each branch of the merger tree starts at a progenitor mass of M_{min} and merges at a redshift $z \geq 0$ with the main progenitor branch. Initially, each halo is occupied by hot primordial gas which is captured in the potential well of the halo and shock heated to its virial temperature $T_{vir} = 35.9[V_c/(\mathrm{km\,s^{-1}})]^2$ K, where V_c is the circular velocity of the halo (White & Frenk 1991, K99). Subsequently, this hot gas component is allowed to radiatively cool and settles down into a rotationally supported gas disc at the centre of the halo, which we identify as the central galaxy (e.g. Silk 1977; White & Rees 1978; White & Frenk 1991). The rate at which hot gas cools down is estimated by calculating the cooling radius inside the halo using the cooling functions provided by Sutherland & Dopita (1993) and the prescription in S01 assuming the gas density profile follows that of the hosting dark matter at all times. At early times and in low-mass haloes the cooling times of the gas are much shorter than the halo dynamical time suggesting that no stable shock will exist at the virial radius of the halo, and that the gas does not shock-heat to virial temperature (Birnboim & Dekel 2003; Kereš et al. 2005). We capture this situation by calculating the radiative cooling time of the halo gas under the assumption of it being at virial temperature and comparing it to the halo dynamical time. Whichever is longer will be used to calculate the cooling rate/accretion rate of gas on to the central galaxy. This procedure has been shown to provide an accurate distinction between haloes with shock heated gas and without around a halo mass scale of $\sim 10^{12}$ M$_\odot$ (Croton et al. 2006; Khochfar & Ostriker 2008). Haloes more massive than this show at $z \gtrsim 2$ signs of accretion of cold gas along cosmic filaments (Ocvirk, Pichon & Teyssier 2008; Dekel et al. 2009a), which is not captured within the above modelling approach. We here include the approach of Khochfar & Silk (2009b) that models this behaviour and is based on fits to the results from numerical simulations by Kereš et al. (2009). In Fig. 1 we show the distribution of accretion rates on to central galaxies in a halo of $M_{DM} \sim 10^{12}$ M$_\odot$ at $z = 2.5$. The distribution is in good agreement with the results from fully numerical simulations presented in Dekel et al. (2009a).

In the case of a merger between haloes we assume that all of the hot gas present in the progenitors is shock heated to the virial temperature of the remnant halo, and that gas can only cool down on to the new central galaxy which is the central galaxy of the most massive progenitor halo. The central galaxy of the less massive halo will become a satellite galaxy orbiting inside the remnant halo. In
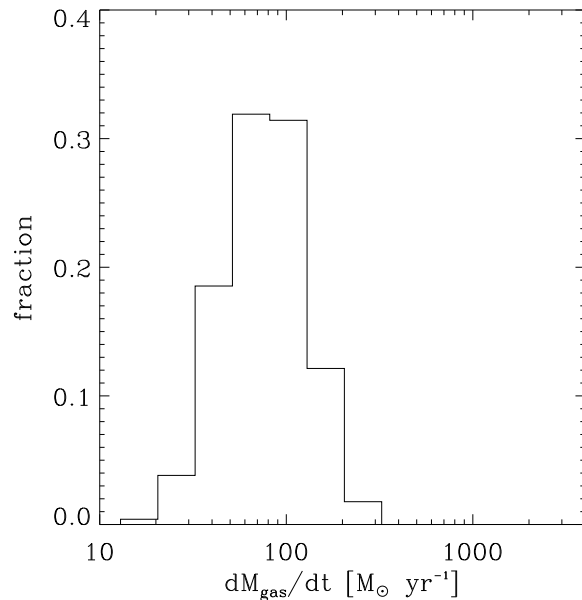
Figure 1. The distribution of SAM accretion rates of cold gas on to central galaxies living in haloes with $M_{DM} \sim 10^{12}$ M$_\odot$ at $z = 2.5$. The distribution is in good agreement with the results from fully numerical simulations presented in Dekel et al. (2009a). We do not include major mergers in this plot due to the ambiguity of the time-scale over which the gaseous material of the satellite galaxy contributes to the central galaxy. The missing mergers explain the slight mismatch at high accretion rates with Dekel et al. (2009a).

this way, a halo can host multiple satellite galaxies, depending on the merging history of the halo, but will always only host one central galaxy on to which gas can cool. The cold gas content in satellite galaxies is given by the amount present when they first became satellite galaxies and does not increase, instead it decreases due to ongoing star formation and supernova feedback (see however e.g. Khochfar & Ostriker 2008; Kang & van den Bosch 2008, for models on gradual gas stripping).

In the simplified picture adopted above, the amount of gas available to cool down is only limited by the universal baryon fraction. However, in the presence of a photoionizing background the fraction of baryons captured in small haloes is reduced (Gnedin 2000) and we use the recipe of Somerville (2002), which is based on a fitting formula derived from hydrodynamical simulations by Gnedin (2000), to estimate the amount of baryons in each halo. For the epoch of reionization, we assume $z_{reion} = 10$, based on recent results from *Wilkinson Microwave Anisotropy Probe* (Komatsu et al. 2011).

2.2.2 Cooling shut-off mass scale

Cooling rates for massive galaxies must drop off significantly in order to e.g. reproduce the observed colour distribution and mass function of galaxies (e.g. Croton et al. 2006). Possible candidates for physical processes responsible in shutting down cooling in massive dark matter haloes are e.g. active galactic nuclei feedback (e.g. Granato et al. 2004; Croton et al. 2006; Bower et al. 2006) or gravitational heating by infalling sub-structures (Khochfar & Ostriker 2008; Dekel & Birnboim 2008; Johansson, Naab & Ostriker 2009). Effectively, these processes result in cooling being suppressed in haloes above a critical mass scale, and have been implemented using a cooling shut-off in haloes above a critical circular velocity (K99) or mass scale (Cattaneo et al. 2006). By applying an effective

shut-off mass scale of $M_{\rm DM,crit} \approx 10^{12}\,{\rm M}_\odot$ at $z \lesssim 2$ one is able to reproduce the colour distribution and mass function of galaxies (Cattaneo et al. 2006). Additionally, such models are able to reproduce the frequency of dry, gas-poor, major mergers (Khochfar & Silk 2009a). In the following we will modify our fiducial cooling model as laid out in Section 2.2.1 by adopting a quenching of cooling in dark matter haloes above a critical mass scale of $M_{\rm DM,crit} \geq 2.5 \times 10^{12}\,{\rm M}_\odot$ at $z \leq 2$ which is similar to the value proposed in Cattaneo et al. (2006) ($M_{\rm DM,crit} \geq 2 \times 10^{12}\,{\rm M}_\odot$), and allows us to have gas in massive late-type galaxies (see Fig. 4). Note that we allow the gas that is already in the disc of a galaxy to continue forming stars until it is used up, even after the host halo is more massive than $M_{\rm DM,crit}$.

2.2.3 Star formation in discs and supernova feedback

Once cold gas has settled down in a disc, we allow for fragmentation and subsequent star formation according to a parametrized global Schmidt–Kennicutt type law (Kennicutt 1998) of the form $\dot{M}_* = \alpha M_{\rm gas}/t_{\rm dyn,gal}$, where α is a free parameter describing the efficiency of the conversion of cold disc gas $M_{\rm gas}$ into stars, and $t_{\rm dyn,gal}$ is the dynamical time of the galaxy and is approximated to be $1/10$ times the dynamical time of the hosting dark matter halo (Mo, Mao & White 1998, K99). For a satellite galaxy we calculate the dynamical time using the halo properties when it last was a central galaxy. We assume here that newly formed stars $\dot{M}_*$ all contribute to the stellar disc $M_{\rm disc}$ of the galaxy.

Feedback from supernovae plays an important role in regulating star formation in small mass haloes and in preventing too massive satellite galaxies from forming (Dekel & Silk 1986; Khochfar et al. 2007). We implement feedback based on the prescription presented in K99 with

$$\Delta M_{\rm reheat} = \frac{4}{3}\epsilon \frac{\eta_{\rm SN} E_{\rm SN}}{V_{\rm c}^2} \Delta M_*. \tag{1}$$

Here, we introduce a second free parameter ϵ which represents our lack of knowledge on the efficiency with which the energy from supernovae reheats the cold gas. The expected number of supernovae per solar mass of stars formed for a typical IMF (e.g. Scalo) is $\eta_{\rm SN} = 5 \times 10^{-3}$, and $E_{\rm SN} = 10^{51}$ erg is the energy output from each supernova. We take $V_{\rm c}$ as the circular velocity of the halo in which the galaxy was last present as a central galaxy or is right now.

2.2.4 Implementation

In between mergers the evolution of galaxies is governed by the equations presented in the previous sections. We solve this coupled system of differential equations by integration in between time-steps of constant $\Delta z = 0.02$, during which the halo properties are kept fixed. We thus solve following set of equations:

$$\dot{M}_* = \alpha \frac{M_{\rm gas}}{t_{\rm dyn,gal}}$$

$$\dot{M}_{\rm reheat} = \frac{4}{3}\epsilon \frac{\eta_{\rm SN} E_{\rm SN}}{V_{\rm c}^2} \dot{M}_*$$

$$\dot{M}_{\rm gas} = \dot{M}_{\rm cool} - \dot{M}_{\rm reheat} - \dot{M}_*$$

$$\dot{M}_{\rm hot} = -\dot{M}_{\rm cool} + \dot{M}_{\rm reheat}$$

$$\dot{M}_{\rm disc} = \dot{M}_*. \tag{2}$$

Here $\dot{M}_{\rm cool}$ is the cooling rate applying the prescriptions of the previous sections. The above set of equations is strictly only applicable to central galaxies, which show cooling of hot gas. For satellite galaxies we use a modified set of equations with $\dot{M}_{\rm hot} = M_{\rm hot} = \dot{M}_{\rm cool} = 0$. All gas that is reheated in satellites is added to the hot gas reservoir of the central galaxy.

2.2.5 Galaxy mergers and bulge formation

We allow for mergers between galaxies residing in a single halo. As mentioned earlier, each halo is occupied by one central galaxy and a number of satellite galaxies depending on the past merging history of the halo. Whenever two haloes merge, the galaxies inside them will merge on a time-scale which we calculate by estimating the time it would take the satellite to reach the centre of the halo under the effect of dynamical friction. Satellites are assumed to merge only with central galaxies and we set up their orbits in the halo according to the prescription of K99, modified to use the Coulomb logarithm approximation of S01 and the correction factor of Jiang et al. (2008). Expressed in units of the Hubble time the dynamical friction is only dependent on the mass ratio of the merging partners. The merger rates in our SAM are in good agreement with observations (Jogee et al. 2009) and agree within a factor of few with other models (Hopkins et al. 2010a,b).

We do not distinguish between the effects of major $R \equiv M_{\rm gal,1}/M_{\rm gal,2} \leq 3.5$ ($M_{\rm gal,1} \geq M_{\rm gal,2}$) and minor mergers $10 > R > 3.5$ in our SAM, but rather apply a model that shows a smooth transition between the effects of such mergers. In what follows the index 1 will always refer to the primary galaxy and the index 2 to the merging satellite galaxy. During major mergers the stellar discs of the progenitors will be almost completely destroyed and added to the bulge component of the remnant. In practice we assume that the amount of disc mass scattered into the bulge is $\min[M_{\rm disc,1}, M_{*,2}]$ (Hopkins et al. 2009a). In addition we assume that a starburst will be triggered due to the interaction of the galaxies. The fraction of cold disc gas transformed into stars during the starburst is modelled using a function $f_{\rm burst}$ that includes dependencies on the cold gas fraction $f_{\rm gas} \equiv M_{\rm gas}/(M_{\rm gas} + M_*)$, the disc fraction $f_{\rm disc} \equiv M_{\rm disc}/M_*$ and mass ratio R of the merging galaxies (Hopkins et al. 2009a). We here use the following functional form that shows broad agreement with results from detailed numerical merger simulations (Hopkins et al. 2009a).

$$f_{\rm burst} = 1 - (1 + r_{\rm sb}/r_{\rm disc}) \exp(-r_{\rm sb}/r_{\rm disc}). \tag{3}$$

We calculate the disc scalelength $r_{\rm disc}$ using the disc model of Mo et al. (1998) and the radius $r_{\rm sb}$, within which gas loses its angular momentum and contributes to the central starburst via:

$$r_{\rm sb} = \alpha_{\rm sb}(1 - f_{\rm gas}) f_{\rm disc} F_\theta G(R), \tag{4}$$

with $G(R) \equiv 2R/(1 + R)$. We set the numerical constant $\alpha_{\rm sb} = 1$ and the orbit-dependent constant $F_\theta = 1.2$ (Hopkins et al. 2009a). The latter represents an average value for a range of different merging orbits.

The cold gas that is not converted into stars during the merger is added to the gaseous disc of the remnant. This results in following composition for the remnants of major and minor mergers:

$$M_{\rm bul,rem} = M_{\rm bul,1} + M_{\rm bul,2} + \min[M_{\rm disc,1}, M_{*,2}]$$
$$\qquad + M_{\rm disc,2} + f_{\rm burst,1} M_{\rm gas,1}$$
$$\qquad + f_{\rm burst,2} M_{\rm gas,2} \tag{5}$$

$$M_{\rm disc,rem} = M_{\rm disc,1} - \min[M_{\rm disc,1}, M_{*,2}] \tag{6}$$

$$M_{\mathrm{gas,rem}} = (1 - f_{\mathrm{burst},1})(M_{\mathrm{gas},1})$$
$$+ (1 - f_{\mathrm{burst},2})M_{\mathrm{gas},2}. \qquad (7)$$

Immediately after major mergers our model galaxies have a large fraction of their stars in the bulge component and the stellar disc can start re-growing by either conversion of cold gas that was not used up in the merger or freshly accreted gas. We here assume mergers as the only efficient means of bulge formation and neglect other possible secular effects such as e.g. disc instabilities (see e.g. Combes 2009).

3 MODEL NORMALIZATION

The various prescriptions for physical process introduced in the last section include a number of free parameters which represent our lack of knowledge on parts of the underlying physical processes. Generally SAMs use a set of observations to fix these parameters. Reproduction of such observations thus cannot be seen as a model prediction but rather a 'tuning' of it. In this section we present the core observations our free parameters are tuned to and their individual values. A summary of these values is given in Table 1.
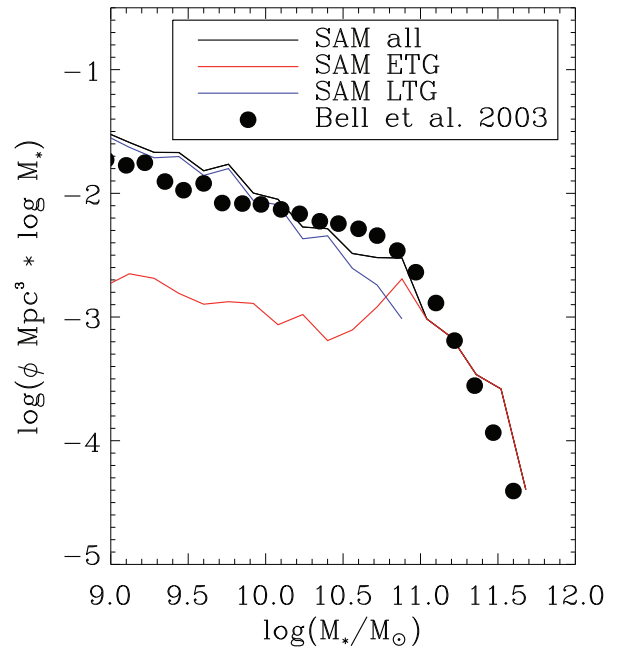
3.1 Mass function

The mass function of galaxies is a core observable that is well measured and robust. Much progress in galaxy modelling has been achieved over the last years by focusing on reproducing specific features in it such as e.g. the steep exponential decline at high masses (Benson et al. 2003; Croton et al. 2006; Khochfar & Ostriker 2008) or the steepness of the faint-end slope as a function of redshift (Khochfar et al. 2007). The ATLAS^{3D} parent sample (Paper I) shows very good agreement with the mass function of Bell et al. (2003), to which we compare our best-fitting $z = 0$ model mass function (Fig. 2). We find very good agreement both in shape and in overall normalization over a wide range in masses, in particular at the high-mass end, where our model population is dominated by ETGs with bulge-to-total mass ratios $(B/T) \gtrsim 0.7$ (see Fig. 3).

3.2 Bulge-to-total mass ratios

Continued merging is transforming morphologies of galaxies by scattering disc stars into bulges. If modelled correctly, the observed trend of increasing bulge fractions with galaxy mass should be recovered by the model. Since we focus here on ETGs this is an important test. In Fig. 3 we show the B/T and stellar masses of our model galaxies, as well as the median B/T at a given mass. We are able to recover the general observed trend towards bulge-dominated systems with increasing mass. The median B/T is below 0.2 for galaxies with $M_* \lesssim 5 \times 10^{10}\,\mathrm{M_\odot}$ and makes a strong transition to $B/T > 0.6$ at $M_* \gtrsim 10^{11}\,\mathrm{M_\odot}$. It appears when the cooling of gas starts slowing down, in haloes below $M_{\mathrm{DM,crit}}$. As a consequence

Figure 2. The mass function of galaxies at $z = 0$ in our best-fitting model (solid line). Filled circles are measurements by Bell et al. (2003). Red and blue lines show the early-type and late-type galaxy mass function, respectively.

discs grow slower, while merging continues to transform discs into spheroids, shifting the median B/T to larger values.
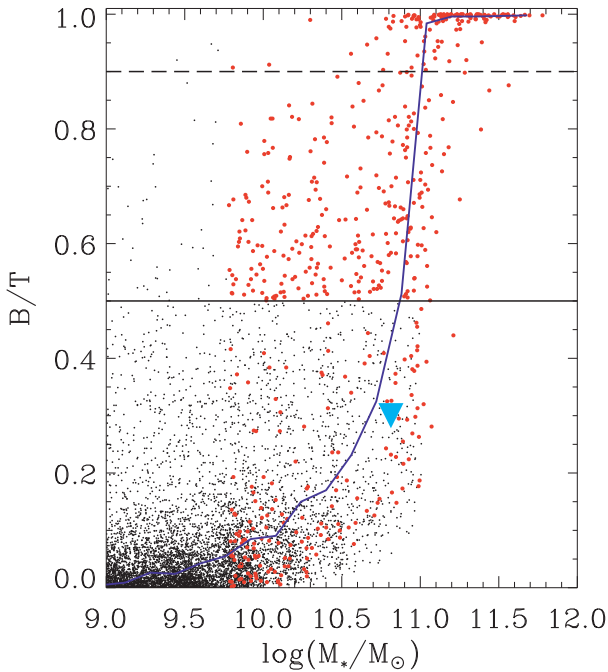
3.3 Gas fraction

Another important quantity related to the efficiency of disc re-growth and survival during mergers is the cold gas fraction, $f_{\mathrm{gas}} \equiv M_{\mathrm{gas}}/(M_{\mathrm{gas}} + M_*)$, as a function of the stellar mass. We show the median value from our model for late-type galaxies with $B/T < 0.5$ in Fig. 4, and compare it to the observed range in disc galaxies (Bell & de Jong 2001; Kannappan 2004; McGaugh 2005). We find fair agreement for model galaxies with $M_* > 10^9\,\mathrm{M_\odot}$ and the observations. The decreasing gas fraction in our model is mainly due to the increasing cooling time as a function of host halo mass, and the sharp cooling shut-off in haloes above $M_{\mathrm{DM,crit}}$.

3.4 Early-type classification

In general, SAMs separate between ETG and late-type galaxies using the B/T either in mass or in B-band magnitude (e.g. K99; S01; Bower et al. 2006). This approach is based on the good correlation between the Hubble T-type and the B-band B/T of galaxies (Simien & de Vaucouleurs 1986). The ETGs selected within the ATLAS^{3D} survey are in very good agreement with morphologies based on the T-type classification scheme (Paper I). We will use here a fiducial value for the bulge-to-total mass ratio of $B/T = 0.5$ to separate ETG from late-type galaxies.

The ATLAS^{3D} survey, however, contains a significant numbers of flat disc-like galaxies that have morphologies similar to late-type spirals, but do not show evidence for gas, dust or spiral arms, and are for this reason classified as early-types (hereafter Paper VII Cappellari et al. 2011b) according to the standard morphological

Table 1. Most important free model parameters and their adopted values.

Star formation efficiency	α	0.02	Section 2.2.3
Supernovae feedback efficiency	ϵ	0.4	Section 2.2.3
Minimum gas fraction in late-types	f_{red}	0.15	Section 3.4
Early-type threshold	f_{early}	0.5	Section 3.4
Fast rotator threshold	f_{fast}	0.1	Section 4.1

Figure 3. B/T of galaxies as a function of mass. The solid blue line shows the median value at a given galaxy mass. Our results show a clear trend towards bulge-dominated galaxies at larger masses. The overall scatter of the distribution is largest around 10^{11} $M_\odot$, which also marks the point at which the galaxy populations is largely dominated by ETGs. The solid triangle shows the Milky Way value of Smith et al. (2007). The horizontal solid and dashed lines mark the transition to ETGs ($f_{early} = 0.5$) and slow rotators ($f_{fast} = 0.1$), respectively. Large red circles show the final extended ETG sample in the SAM, including the additional criterion $f_{red} = M_{gas}/M_* = 0.15$, on the minimum gas fraction in late-type galaxies. The latter has been included to mimic the ATLAS^{3D} selection of ETGs, which allows for the inclusion of gas-poor low B/T galaxies.

classification (Sandage 1961). Such *red* spirals are classified as fast rotators (Paper III; Krajnović et al. 2011, hereafter Paper II) and are not included if the early-type selection in the SAM is done purely based on a B/T cut. The combination of a strong decline in the mass function of galaxies and the transition from fast to slow rotator dominance suggest that the impact on the ratio of fast to slow rotators by missing such galaxies could be important at masses $\gtrsim 10^{11}$ $M_\odot$ (Paper III). We address this issue by including an additional criterion based on the gas fraction in galaxies with low B/T. We first compare the distribution of the cold H I gas fraction $f_{red} \equiv M_{gas}/M_*$ in model central galaxies with that obtained from the ATLAS^{3D} sample (Sarra et al., in preparation) assuming a constant molecular-to-atomic ratio (see however Obreschkow et al. 2009, for more detailed modelling of the molecular fraction in cold gas). The distributions show very similar trends with a peak at high gas fractions for late-type galaxies and ETGs spanning a wide range from low to high gas fractions with a strong tendency for low gas fractions (Sarra et al., in preparation). Modelled late-type galaxies ($B/T < 0.5$) show in addition a small peak at gas fractions below ∼15 per cent which is not seen in the observations. Such galaxies are likely candidates for fast rotators with low B/T and we therefore adopt an additional criterion for ETGs with $B/T < 0.5$ and $f_{red} < 0.15$. A significant fraction of galaxies with masses ∼$10^{11} M_\odot$ in our model are centrals living in haloes which have been crossing $M_{DM,crit}$ some time ago, and since then did not encounter any significant mergers, thus using up their gas reservoir and building a stellar disc with little
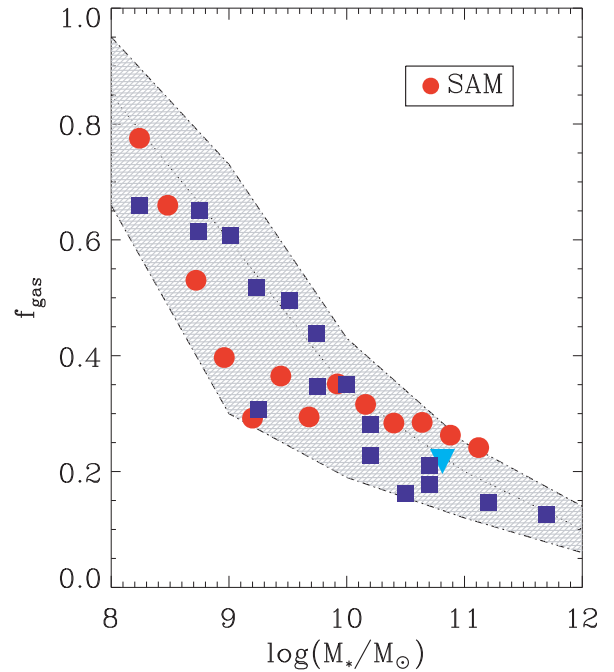
Figure 4. The median fraction of gas $f_{gas} = M_{gas}/(M_{gas} + M_*)$ as a function of galaxy mass in the SAM (filled circles) range covered by observations including their error bars (hatched region). Solid squares show the compilation of various observational data (Bell & de Jong 2001; Kannappan 2004; McGaugh 2005), and the solid triangle is the value for the Milky Way. The declining gas fraction with stellar mass is mainly due to the increasing cooling time-scales for the gas. Due to the sharp cooling shut-off in haloes above $M_{DM,crit}$ the gas fraction declines very sharply to zero.

interference. The hosting halo of these galaxies are not very much larger than $M_{DM,crit}$, thus explaining why they do not reach masses larger than ∼10^{11} $M_\odot$. In general, we find that the majority of low B/T fast rotators below ∼$10^{11} M_\odot$ are satellite galaxies. The fraction of ETGs is known to increase with the density of the environment (Dressler 1980). A consistent trend has been found for the galaxies in the ATLAS^{3D} survey (Paper VII). To include to the first order gas-poor low B/T satellite galaxies in high-density environments, we add satellite galaxies in group-like dark matter haloes with $M_{DM} \gtrsim 4 \times 10^{13} M_\odot$ and stellar masses larger than $10^{10} M_\odot$. Again, we here use the early-type definition with $B/T < 0.5$ and $f_{red} < 0.15$ for these satellite galaxies. We find that the trend in the ratio of fast to slow rotators is not significantly affected by adding the satellite population, as most of them have masses in a range where fast rotators clearly dominate the population of ETGs.

In Fig. 3, we show the final selection of ETGs from the overall model sample. This selection yields a total number density of 1.6×10^{-3} Mpc^{-3} ETGs with $M_* \geq 6 \times 10^9 M_\odot$, which is in good agreement with the observed value for the ATLAS^{3D} sample of 2.2×10^{-3} Mpc^{-3} (Paper I). In Fig. 2 we show the mass function separated into ETG and late-type galaxies for our adopted selection. The high-mass end is as expected dominated by ETGs, and we find that the number density is nearly constant for $M_* < 10^{11} M_\odot$. Compared to the observed mass function presented in Paper I our model produces too few ETGs at low masses, most of which should be fast rotators and too few very massive $M_* > 10^{11} M_\odot$ late-type galaxies.

Approximately 80 per cent of the model ETGs have $B/T > 0.5$ while the remaining 20 per cent are low B/T galaxies devoid of gas.

4 FAST- AND SLOW-ROTATING ELLIPTICAL GALAXIES

The results of the ATLAS[3D] survey suggest that ETGs can be classified into two classes based on the parameter $\lambda_R \equiv \langle R\,|V|\rangle/\langle R\sqrt{V^2+\sigma^2}\rangle$ which has been shown to be a good proxy for the specific baryonic angular momentum in ETG (Paper III; Emsellem et al. 2007; Jesseit et al. 2009). Using a suite of high-resolution simulations, Paper VI shows that during major mergers ($R < 2$) of late-type galaxies the geometry of the encounter is the dominant factor in deciding whether the remnant is a slow or fast rotator. In general, major mergers that are retrograde (prograde) with respect to the main progenitor result in slow (fast) rotators. In minor mergers ($R \geq 3$) remnants are almost exclusively fast rotators. However, the situation is not as simple as that. Simulated slow rotators tend in general to be too flat compared to observed ones and have properties similar to 2σ galaxies (Paper II), suggesting that a single major merger might not be the way to form them. Furthermore, merging of remnants shows that the orbital angular momentum is able to spin-up slow rotators, even in major mergers. Thus, to predict the proper outcome of a binary merger, one needs to know the initial state of the progenitors in terms of their angular momentum and how the orbital angular momentum is re-distributed within the remnant. Ideally, one would follow individual galaxies and calculate the change in λ_R due to mergers and star formation in discs, the latter generally contributing to an increase in λ_R.

To assess the impact of mergers on the evolution of λ_R one can to the first order use the analogy to dark matter haloes and their spin parameter λ (Emsellem et al. 2007). Following the merging history of dark matter haloes, and under the assumption of random orbits and complete transfer of orbital angular momentum to the remnant, one recovers a lognormal distribution for λ consistent with results from cosmological simulations (Maller, Dekel & Somerville 2002). The distribution of λ in dark matter haloes shows only a weak mass dependence (Bett et al. 2007), in stark contrast to the strong mass dependence of λ_R in ETGs implying that whatever drives the trend in λ_R with mass is not just simple transfer of orbital angular momentum. While individual mergers might burst or lower λ_R occasionally based on the orbit (Paper VI), continuous merging on random orbits will drive λ_R to a mass-independent distribution at a median value of $\lambda_R \sim 0.038$ (Maller et al. 2002). Here, we used the relation between the spin parameter λ and λ_R presented in Emsellem et al. (2007) and the median spin parameter of dark haloes in Bett et al. (2007). Such low λ_R values would classify the majority of ETGs as slow rotators, thus additional physical processes need to be important.

Detailed kinematic analyses of ATLAS[3D] galaxies by Paper II show that a large fraction of fast rotators have disc-like regular rotation patterns and bars, suggesting that the stellar body is hosting a disc component. Stellar discs in terms of λ_R would all be classified as a fast-rotating component (Paper VI). If mergers indeed on average lead to low λ_R, the presence of a disc can be all that makes the difference between fast and slow rotators. The process of disc building (increasing λ_R) is in direct competition with the process of disc destruction by mergers (lowering λ_R).

Motivated by above arguments we introduce a simple model based on the mass fraction in discs to investigate the origin of fast- and slow-rotating ETGs. In what follows we choose the fraction of fast rotators as a function of luminosity as our key observable, and gauge our models against it.
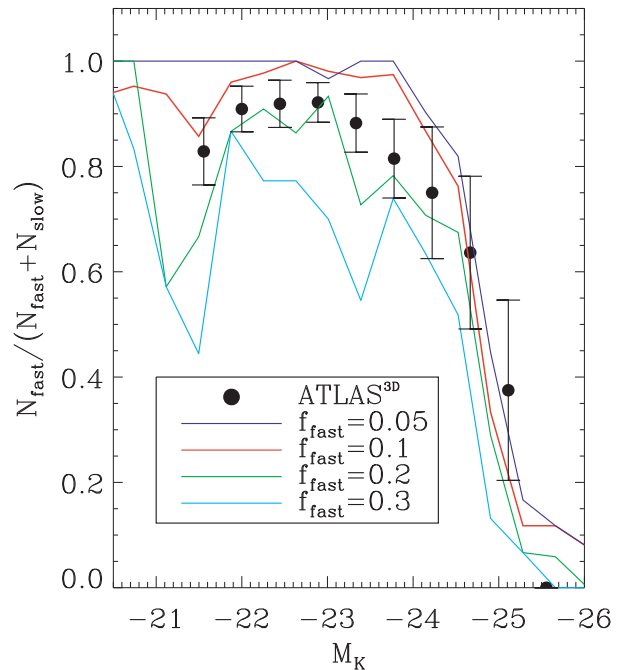
Figure 5. The fraction of fast rotators in the overall population of ETGs in the ATLAS[3D] sample (filled symbols) (Paper III). The SAM outputs for different values of f_{fast} are shown as different coloured solid lines. Throughout this paper we will use as our fiducial value for the minimum disc fraction in fast rotators $f_{fast} = 0.1$.

4.1 Fast rotators

Fast rotators are the majority of ETGs and dominate the population at $M_K \gtrsim -24$ (see Fig. 5). Detailed analyses of several fast rotators by Krajnović et al. (2008) and Paper II reveal the existence of disc-like features in early-type host galaxies in agreement with earlier studies of Rix & White (1990). We here assume in agreement with Paper VII that such stellar discs are present in all fast rotators and use their existence as our criterion to distinguish between fast and slow rotators. We introduce a free model parameter f_{fast} that gives the lower limit to the disc mass in fast rotators. Every early-type model galaxy with a disc fraction $M_{disc}/M_* < f_{fast}$ is classified as a slow rotator. We calculate K-band magnitudes for our model galaxies using their star formation history and the stellar population synthesis models of Bruzual & Charlot (2003). In Fig. 5 we show the fraction of fast rotators in the overall population of ETGs as a function of their rest-frame K-band magnitude for the ATLAS[3D] sample. The sample shows a clear trend towards slow rotators at the luminous end and is dominated over the remaining observed range by fast rotators (Paper III). We show the fraction of fast rotators from our SAM for different values of the free parameter f_{fast}. In general we find that values of $f_{fast} \sim 0.1$–0.15 show good agreement with the observations. We here choose $f_{fast} = 0.1$ as our fiducial value, based on matching the observational data in Fig. 5 and the additional constraint of being close the number density of fast and slow rotators from the ATLAS[3D] sample (see Fig. 11). The exact value of f_{fast} does not influence the shape of the curve shown in Fig. 5, it only changes the magnitude at which fast rotators start to dominate. The modelled galaxy population of fast and slow rotators is in good agreement with the observations, supporting the idea that stellar discs are the dividing factor between fast and slow rotators.

The formation path towards fast-rotating ETGs in our model is either by rebuilding a stellar disc around a spheroid, the growth of a spheroid via the destruction of existing discs in late-type galaxies or the exhaustion of gas in late-type galaxies. Slow rotators on the other hand have two possible formation paths: major mergers or repeated dry minor mergers. In what follows we will investigate the importance of these different paths by changing the model prescription within our fiducial SAM. We will focus in particular on the importance of gas cooling, the destruction of stellar discs in major mergers, starburst during major mergers and the effects of minor mergers.

4.1.1 Impact of gas cooling

We first change our fiducial model in a way that highlights the importance of gas cooling for the formation of fast rotators. We will call it *max-merg* in the following (label *MM* in Figs 6 and 7). In this model every binary major merger with $R \leq 3.5$ results in a slow rotator, and all the progenitor disc mass is added to the bulge, as well as all progenitor gas is converted into bulge stars during a starburst. The modification to the fiducial model (equation 5) is summarized below. For major mergers we assume

$$M_{\mathrm{bul,rem}} = M_{\mathrm{bul,1}} + M_{\mathrm{bul,2}} + M_{\mathrm{dis,1}} + M_{\mathrm{dis,2}}$$
$$+ M_{\mathrm{gas,1}} + M_{\mathrm{gas,2}}$$
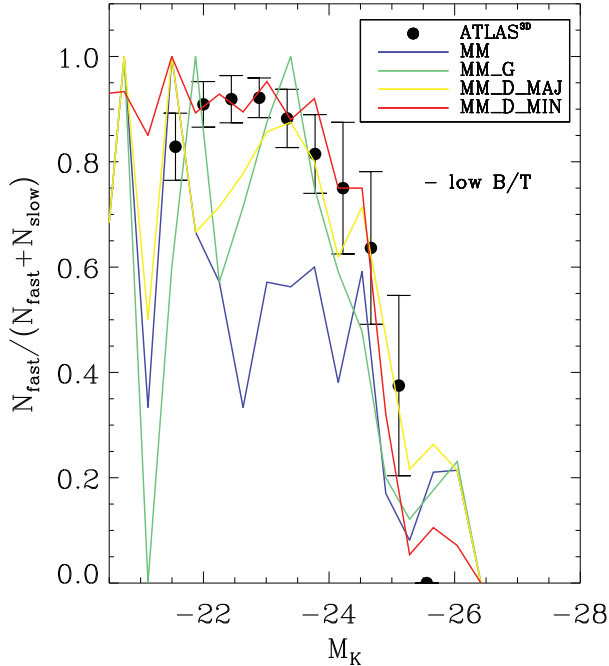
Figure 6. The fraction of fast rotators in the overall population of ETGs in the ATLAS[3D] sample (filled symbols) (Paper III). The SAM outputs for different model assumptions are shown by the various lines in the figure (see the text for details on the models). For all models we use $f_{\mathrm{fast}} = 0.1$. The blue, green and yellow lines show models including the effects of major mergers only, while the red line shows the outcome for a model including minor mergers. Results in this figure are shown for fast rotators that do not have $B/T < 0.5$ ($- low B/T$). The survival of stellar and gaseous discs during major mergers (models MM_D_MAJ and MM_G, respectively) plays mostly a role for fast rotators around $M_K \sim -23$, while the overall population of fast rotators is dominated by regrowth of a disc from gas cooling and disc destruction in minor mergers.
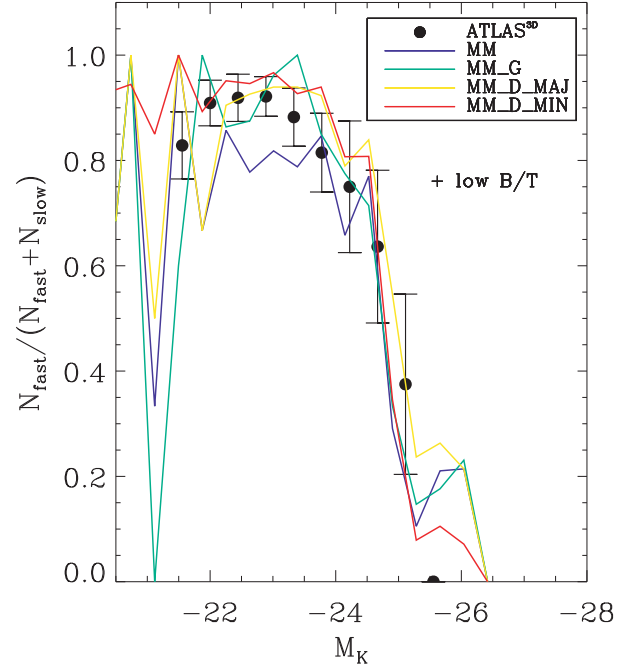
Figure 7. Same as Fig. 6 but now including the contribution from gas-poor low B/T galaxies (+ *low B/T*). Such galaxies play an important role in major merger only models. However, in the model including the effect of minor mergers (MM_D_MIN) the fraction of fast rotators originating from drying out of late-type galaxies in high-density environments is significantly lowered.

$$M_{\mathrm{dis,rem}} = 0$$
$$M_{\mathrm{gas,rem}} = 0 \tag{8}$$

and for minor mergers with $10 \geq R > 3.5$:

$$M_{\mathrm{bul,rem}} = M_{\mathrm{bul,1}} + M_{*,2}$$
$$M_{\mathrm{dis,rem}} = M_{\mathrm{dis,1}}$$
$$M_{\mathrm{gas,rem}} = (M_{\mathrm{gas,1}} + M_{\mathrm{gas,2}}). \tag{9}$$

In this model the formation of fast rotators via discs is maximally hindered and only allowed via cooling of gas from the hot halo and cold gas from gas-rich satellites in minor mergers. The solid blue line in Fig. 6 shows the fraction of fast rotators that formed via disc growth around bulges. We find the expected trend of this mode being more important at lower mass scales, when cooling times are shorter, most visible at $M_K \gtrsim -24$. However, shorter cooling times also mean that more gas will have cooled down before a merger takes place, and thus less material is available to re-grow a disc. For massive galaxies one can use a rough estimate to evaluate the role of cooling with respect to mergers. Observations of the merger rate in the nearby Universe find on average 0.0001 Gyr^{-1} Mpc^{-3} mergers for massive galaxies with $M_* > 2.5 \times 10^{10}$ M$_\odot$ (Jogee et al. 2009). For the ATLAS[3D] early-type sample this suggests less than one merger within the last Gyr per galaxy. Cooling time-scales on the other hand are around 1 Gyr (Neistein & Weinmann 2010), suggesting that cooling processes and associated star formation in disc-like components are not negligible in between merger events. However, cooling by itself is not sufficient to produce enough fast rotators by means of transforming bulge-dominated major merger remnants as evidenced by the large drop in the fast rotator fraction at $M_K \gtrsim -24$. The more important contribution to the fraction of fast rotators comes from gas-poor low B/T satellite galaxies

living in dense environments (see Fig. 7). On average, fast rotators that are 'dried-up' late-type galaxies in the range $-22 > M_K > -25$ are nearly three times more frequent than 're-grown disc' fast rotators showing that disc re-growth after a major merger is a less important channel for the formation of fast rotators than possible environmental effects leading to the exhaustion of gas in late-type galaxies.

4.1.2 Gas-rich mergers

Within our fiducial merger model stellar discs have two distinct origins. They are either the remains of a stellar disc that survived a merger or re-grown from gas that settled into a disc after a merger. The gas for the latter process can be part of the progenitor discs that survived the merger or gas that is radiatively cooling and settling on to a disc. The importance of the latter process has been addressed in the last section and we will turn now to the survival of gas in progenitor discs. Numerical simulations show that during mergers of galaxies with high gas fractions, progenitor discs are able to survive and to start quickly rebuilding stellar discs (Robertson et al. 2006; Hopkins et al. 2009a). Our fiducial merger model in equation (5) does take the results from such simulations into account via the function f_{burst}. In the *max-merg* model above we assumed $f_{burst} = 1$. To estimate the importance that the survival of gaseous disc during major mergers has on rebuilding stellar discs we modify the max-merg model by using f_{burst} from equation (5). The survival of gaseous disc material during mergers is mainly affecting the fraction of fast rotators between $M_K \sim -23$ and $M_K \sim -24$, with only a mild increase in the total number of fast rotators by a factor of 1.6 (see Figs 6 and 7, dotted line, label *MM_G*). From this we conclude that in our model the formation of fast rotators via the growth of stellar discs from cold disc gas that is surviving major mergers is less important than via radiative cooling of gas.

4.1.3 Survival of stellar discs

Detailed numerical simulations of binary galaxy mergers with and without gas show that the mass ratio of the merging partners plays a crucial role in erasing the memory of the progenitor's stellar disc (e.g. Barnes & Hernquist 1992; Naab & Burkert 2003; Hopkins et al. 2009a). Within our fiducial model we always destroy a fraction of the stellar disc that is given by min $[M_{di,1}, M_{*,2}]$. Effectively, our model states that ten 10:1 mergers have the same effect on a stellar disc as one 1:1 merger (Bournaud, Jog & Combes 2007). To see how the survival of a stellar disc will influence the fraction of fast rotators we modify the max-merg model to include the dependence on the mass ratio as laid out in our fiducial merger model equation (5). We assume that only in major mergers, $R < 3.5$, the disc of the host galaxy will be affected. Minor mergers are neglected in terms of their impact on to the stellar disc, and we will come back to it in the next section. As can be seen from the dashed line labelled *MM_D_MAJ* in Fig. 6, the fraction of fast rotators is mainly increased for luminous galaxies around $M_K \lesssim -23$. This increase is modest with respect to the max-merg model and of the same magnitude as in the case of including stellar disc survival during mergers. Unequal-mass major mergers dominate the overall number of mergers (e.g. Khochfar & Burkert 2001), thus the survival of stellar discs is elevated with respect to the max-merg model. Again, we find that disc re-growth via cooling is more important for the formation of fast rotators after a major merger than the survival of pre-existing properties during this major merger, in this case the stellar disc of the main progenitor.

Our results here and in the previous section show that surviving discs, stellar and gaseous, are important in allowing to maintain and re-grow substantial discs from cooling of gas in ETGs mostly around $M_K \sim -23$, and that the majority of fast rotators are likely to originate from a different formation path within our model which.

4.1.4 Minor mergers

The frequency of minor mergers an ETG encounters during its evolution by far exceeds the number of major mergers (e.g. Khochfar & Silk 2006a; Kaviraj et al. 2009; Naab, Johansson & Ostriker 2009; Shankar et al. 2010). The importance of minor mergers for the formation of bulges in late-type galaxies has been recently pointed out (Weinzirl et al. 2009; Hopkins et al. 2009b) and we here investigate their importance in terms of fast- and slow-rotating ETGs. As discussed above, minor mergers are able to disrupt parts of the stellar disc of their host and to trigger a small starburst (Peirani et al. 2010; Crockett et al. 2011; Kaviraj et al. 2011). We here modify the max-merg model to include the disruption of stellar discs in minor mergers $10 > R > 3.5$, but do not allow for any starburst during it. The solid red line labelled *MM_D_MIN* in Fig. 6 shows the outcome of this model. It is clearly visible how the fraction of fast rotators is significantly increased at $M_K \gtrsim -25$, with respect to the max-merg model. Our results suggest that minor mergers are efficient means in gradually transforming disc-dominated systems into systems with $0.5 < B/T < 0.9$, corresponding to the B/T range of fast-rotating ETGs. As we will show below, the continued impact of such minor mergers is leading to even higher B/T and the formation of slow-rotating ETGs. By comparing Figs 6 and 7 we find that the fraction of fast rotators with such an origin is much larger than the one for fast rotators that are dried up late-type galaxies.

4.2 Slow rotators

Mergers play by construction an important role in the formation of ETGs in our model. Our assumption of equal-mass mergers predominantly resulting in slow rotators is clearly an oversimplification of what is happening in reality (Paper VI). In general, the formation of a slow rotator requires that the orbital angular momentum and the spin of the galaxies compensate each other such that only little angular momentum is left in the remnant, a situation that requires fine-tuning, given that the ratio of orbital angular momentum to spin is on average larger than one (Khochfar & Burkert 2006; Maller et al. 2002) and that slow rotators after one additional major merger tend to spin-up to become fast rotators again (Paper VI). The question thus arises how slow rotators might form in the first place, if even under favourable conditions, such as equal-mass mergers, their formation/survival chances are small (Bois et al. 2010). As we pointed out earlier, minor mergers are very frequent and can contribute a significant fraction of the remnant mass. In an earlier study Khochfar & Silk (2006a) showed that up to 80 per cent of the bulge mass can come from outside the galaxy via mergers, estimates in agreement with numerical simulations of Oser et al. (2010). If this is indeed the case, then slow rotators are the end-stage of constant impact by satellite mergers, falling in from random directions and helping to reduce the angular momentum of the host on average. Since the cooling of gas has mostly ceased in high-mass galaxies living in haloes $> M_{DM,crit}$, disc formation will be terminated as well, and thus the conversion into fast rotators. To highlight the relative importance of minor and major mergers we show in Fig. 8
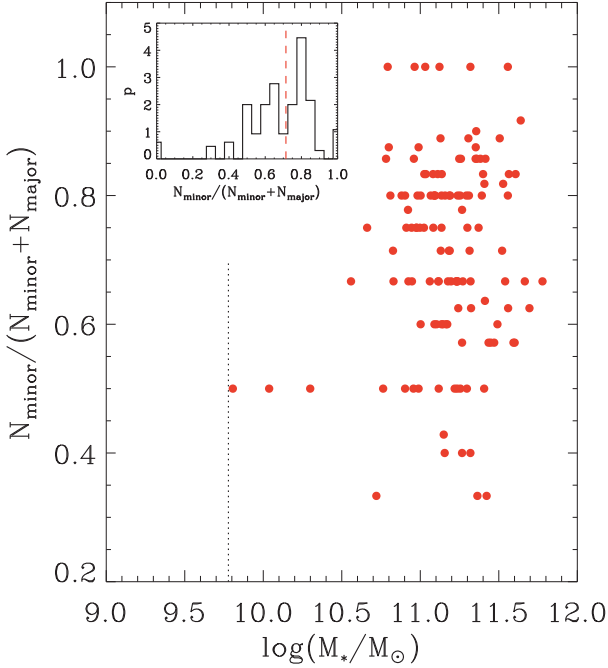
Figure 8. The fraction of minor mergers $N_{minor}/(N_{minor} + N_{major})$ that the most massive progenitor branch of a present-day slow rotator experienced during its evolution. For the sake of better statistics we here define major merger as $R \leq 4$ and minor mergers as $20 \geq R > 4$. The histogram shows the distribution of the minor merger fraction which has a median value of 0.73 (dashed line). Minor mergers clearly dominate the history of slow rotators. However, we do not find a strong correlation with stellar mass. Slow rotators with very few or no major mergers have more minor mergers than slow rotators with some major mergers. The evolution paths of these two classes of slow rotators is very different with the former going through a fast rotator phase, while the latter always stays close to the slow rotator regime. The vertical dotted line shows the completeness limit of the ATLAS^{3D} sample (Paper I).

the fraction of minor mergers that the most massive progenitors of a present-day slow rotators experienced during their evolution. We here define major and minor mergers as $R \leq 4$ and $20 \leq R > 4$, respectively, to increase the statistical significance. There is a large scatter in the fraction of minor mergers that slow rotators experienced during their evolution and no significant correlation with galaxy mass. The median fraction of minor mergers that the most massive progenitor of a slow rotators experiences is ~ 0.7 corresponding to ~ 2.3 more minor than major mergers. The implication of these results is that massive slow rotators had most likely a major merger event in their past, but got constantly hit by minor mergers, that erased any progenitor disc memory and additionally hindered the rebuilding of a sufficiently large stellar disc. Looking at the individual cases of slow rotators in our model, we find that on average slow rotators with high fractions of minor mergers went through an episode in their past during which they were classified as fast rotators, while those slow rotators with low minor merger fractions were always close to the slow rotator regime.

5 FAST AND SLOW ROTATOR DEMOGRAPHICS

The big advantage of the ATLAS^{3D} sample is its completeness, which allows us to directly compare our model population with

the observed one. As we have shown in Fig. 5 our fiducial model is able to reproduce the relative fraction of fast and slow rotators as a function of magnitude. We find in addition that the number density of ETGs with $M_* > 6 \times 10^9 \, M_\odot$ is $1.6 \times 10^{-3} \, Mpc^{-3}$, comparing well to the ATLAS^{3D} one of $2.2 \times 10^{-3} \, Mpc^{-3}$ (Paper I). Approximately 20 per cent of these ETGs are slow rotators, in fair agreement with the 14 ± 2 per cent found in the ATLAS^{3D} sample (Paper III). Having established that our model reproduces the basic statistics of the ATLAS^{3D} sample we can now address the question of what the deciding factors are in the history of an ETG that make it become a fast or slow rotator within our model. As we argued above we take the disc fraction in ETGs to the first order as a proxy of λ_R, thus the balance between disc destruction and formation plays a crucial role.

We start by looking at the fraction of accreted stars that end up in ETGs as a function of their stellar mass. By definition these are all stars that a satellite galaxy contributes to the primary galaxy during a merger and directly proportional to the amount of stellar disc that might be destroyed in the primary (see equation 5), suggesting that fast rotators should have on average $M_{acc}/M_* \leq 0.5$ depending on the amount of gas and stars in the progenitor discs. As demonstrated in Fig. 9, the majority of fast rotators has indeed $M_{acc}/M_* \leq 0.5$ and the amount of accreted material in slow rotators can reach up to 90 per cent of their total mass. These estimates are in agreement with earlier results of Khochfar & Silk (2006a). When dividing the ETG sample
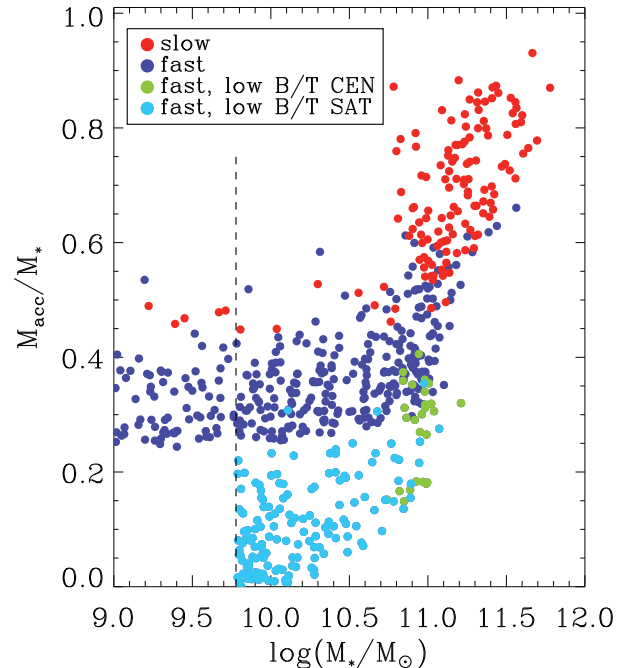
Figure 9. The fraction of accreted stars from satellite galaxies on to ETGs as a function of the present-day galaxy mass. Massive galaxies accrete the majority of their stellar material. This can be up to 90 per cent of the total mass in the most massive galaxies. The population of fast and slow rotators show a clear distinction in this figure, with the latter (red filled circles) showing $M_{acc}/M_* \geq 0.5$. Slow rotators show a strong trend with mass due to the cooling shut-off in haloes more massive than $M_{DM,crit}$. Fast rotators with low B/T ratios are dominantly satellite galaxies in high-density environments that got stripped of their hot haloes and ceased to form stars (light blue filled circles). We do not show satellite galaxies below the ATLAS^{3D} survey mass limit of $\sim 6 \times 10^9 \, M_\odot$ (dashed line), but show central galaxies all the way down to $10^9 \, M_\odot$ to make the trend with mass more visible.

into fast and slow rotators, a clear separation appears supporting the observational classification into slow and fast rotators. Slow rotators have on average larger fractions of accreted material than fast rotators and show a very steep relation between the accreted mass fraction and their total stellar mass.

Fast rotators in our model fall into two different classes, those with $0.5 < B/T < f_{fast}$ (~78 per cent) and those with $B/T \leq 0.5$ and low gas fractions (~22 per cent). The high B/T population shows a clear separation from the other fast rotators, having higher fractions of accreted material at a given stellar mass. Also clearly visible is a moderate correlation with stellar mass towards higher accretion fractions. The low B/T population on the other hand shows a large scatter and stays generally below accretion fractions of 0.3. These two populations in terms of their morphology will not necessarily show different properties other than their B/T ratio, and thus would to the first order look like members of one homogenous class of fast rotators. However, detailed analyses of their stellar population, in terms of age, metallicity and a detailed structure, might reveal differences, due to their different formation paths and/or the environment in which they evolved. As we showed earlier, the most dominant formation channel for fast rotators is via the destruction of existing stellar discs in minor mergers resulting in high B/T fast rotators and possibly thickened stellar discs in contrast to the low B/T population of dried-up late-type galaxies with thin stellar discs.

The trend seen in Fig. 9 can be understood by considering the growth of galaxies. The ratio M_{acc}/M_* increases during dissipation-less mergers and is lowered during dissipational events, like cooling and associated star formation. The modest stellar mass dependence seen for high B/T fast rotators is mainly driven by the slowing down of cooling in massive haloes. Once host haloes reach masses above $M_{DM,crit}$ cooling completely stops and galaxies grow mostly via dissipationless mergers (Khochfar & Silk 2009a) causing the strong dependence of M_{acc}/M_* on stellar mass seen in slow rotators. The low B/T fast rotators resemble the flattened fast rotators in the ATLAS^{3D} sample and are the result of cold star-forming gas running out in either satellites galaxies in dense environments (~17 per cent of fast rotators)(light blue filled circles in Fig. 9) or central galaxies in haloes $> M_{DM,crit}$ that did not experience many mergers during their evolution (~5 per cent) (green filled circles). Another 20 per cent of fast rotators have high B/T ratios and are satellites in dense regions giving a total of ~37 per cent of fast rotators being satellite galaxies subject to environmental effects (Paper I). The majority of ~60 per cent, however, are central galaxies. In contrast, slow rotators are in over 85 per cent of the cases central galaxies.

Besides differences in the fraction of accreted material it is important to ask whether the accreted material is provided in the same way for fast and slow rotators. In Fig. 10 we show the average number of major and minor mergers the most massive progenitor of present-day fast and slow rotators experienced. Not surprisingly, we find that the number of mergers is an increasing function of stellar mass and that the average number of minor mergers is similar for fast and slow rotators of the same mass. The number of major mergers, however, is larger for slow rotators. The average number of major mergers is between 1 and 2, which implies that they encountered at least one major interaction during their formation which would leave its imprint.

In summary, fast and slow rotators mark the transition point in the ability for gas to cool and form stars in discs. Slow rotators have accreted more stars via minor and major mergers, reducing their disc fraction and hence λ_R. In addition, they have more major mergers, at least one on average during their evolution that could leave an imprint in their stellar body.
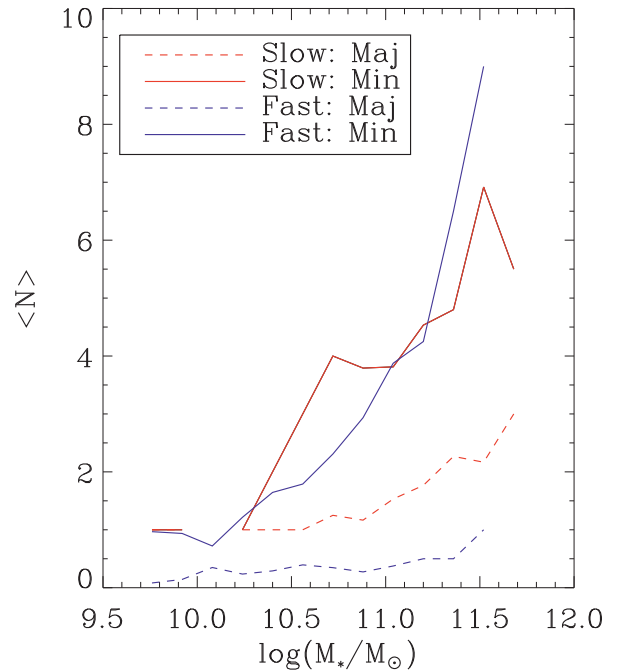
Figure 10. The average number of minor (solid) and major (dashed) mergers that the most massive progenitors of present-day ETGs experience during their evolution. The number of mergers rises with the present-day stellar mass of ETGs. Both populations of ETGs show similar numbers of minor mergers as a function of stellar mass. However, slow rotators have on average more major mergers than fast rotators. The model estimates on the number of mergers is in very good agreement with recent estimates of Conselice & Arnold (2009)

6 THE REDSHIFT EVOLUTION OF FAST AND SLOW ROTATORS

As we mentioned above, in our model the ability to cool gas and the fraction of accreted stars via mergers are important to predict the fraction of fast and slow rotators. The impact of both these physical processes is changing going to higher redshifts. The merger rate of galaxies peaks around $z \sim 2$–3 (e.g. Conselice et al. 2003), and the gas accretion rate also does increase towards higher redshifts (Dekel et al. 2009a). In Fig. 11 we present the number density of fast- and slow-rotating ETGs as a function of redshift for three different ranges in stellar mass ($9.8 \leq \log M_* < 10$; $10 \geq \log M_* < 11$ and $\log M_* > 11$). The horizontal line shows the number density of ETGs in the ATLAS^{3D} volume. Going to higher redshift the number density drops as expected due to the hierarchical build-up of massive galaxies that takes place, and the fact that a larger fraction of massive galaxies are classified as gas-rich late-type galaxies. Independent of the overall decline, the number density of slow rotators in all mass bins in general declines stronger with respect to the one of fast rotators. Many of the slow rotators at a high z are remnants of very recent equal-mass mergers, in contrast to the low-z slow rotators that have had major mergers in their past but are dominated by minor mergers during the later stages of their evolution. As shown by Paper VI, equal-mass mergers that take place under special merger orbits can result in fast rotators. The number densities for slow rotators at high z that we present are therefore upper limits. Independently, our results predict that beyond $z \sim 2$ it will be hard to find slow rotators and that the population of ETGs at $z \sim 2$ should be dominated by fast rotators, which are more than one magnitude more frequent than slow rotators at $M_* > 10^{10} M_\odot$. Taking the observational results
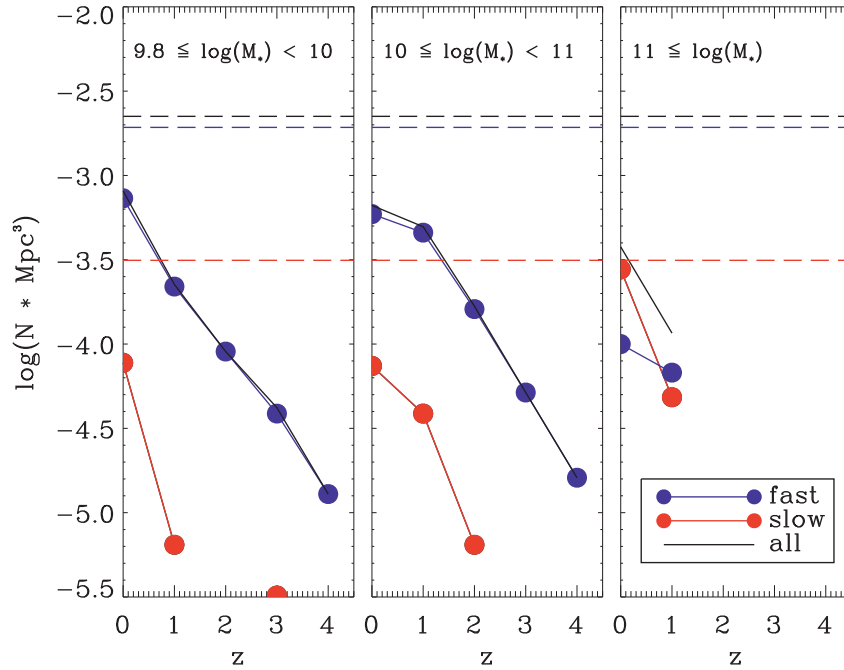
Figure 11. The number density of fast and slow rotators as a function of redshift. We apply three different stellar mass bins to highlight the mass dependence. The long dashed lines show the number density of slow (red), fast (blue) and all (black) ATLAS[3D] galaxies at $z = 0$, respectively. Our model predicts a strong decline of slow rotators even for the highest mass bin and predicts that fast rotators should be more than an order of magnitude more frequent at $z \geq 2$ for galaxies with $M_* > 10^{10} M_\odot$. The high-z number densities of slow rotators are upper limits since they are the results of recent equal-mass mergers that under certain merger orbits result in fast rotators (Paper VI).

on the evolution of the number density of massive ETGs at face value (e.g. Ferreras et al. 2009) our results suggest that basically all massive slow rotators were fast rotators at some point during their evolution.

7 COSMIC VARIANCE

The ATLAS[3D] survey only spans a limited volume of the local Universe within a radius of 42 Mpc. It is thus valid to ask whether cosmic variance has a significant impact on the results of the survey. We try to address this question by using our fiducial model and investigating the effects of cosmic variance using a large-scale N-body simulation.

## 7.0.1 Variations in the dark matter mass function

Depending on the location of a fixed volume within the Universe, the mass function of dark matter host haloes and associated galaxies will change. We estimate this effect by using a cosmological N-body simulation of a $(100 \, \text{Mpc} \, h^{-1})^3$ volume. The particle resolution of the simulation is $10^9 \, M_\odot \, h^{-1}$, and we generate the $z = 0$ mass function for haloes using the FOF algorithm. Fig. 12 shows the mass function of the whole box (red line) and that of 50 randomly placed spherical sub-volumes of the size of the ATLAS[3D] volume. The mass functions agree well at low masses, but starts deviating at large masses due to cosmic variance. To predict the fraction of fast and slow rotators within each of these sub-volumes we take the FOF-mass function and apply the merger-tree algorithm of Somerville & Kolatt (1999) in combination with our fiducial model. We do not construct the merger trees from the simulation, because we do want to also investigate what the impact of randomly generated merger histories is, choosing haloes of the same mass (see Section 7.0.2).
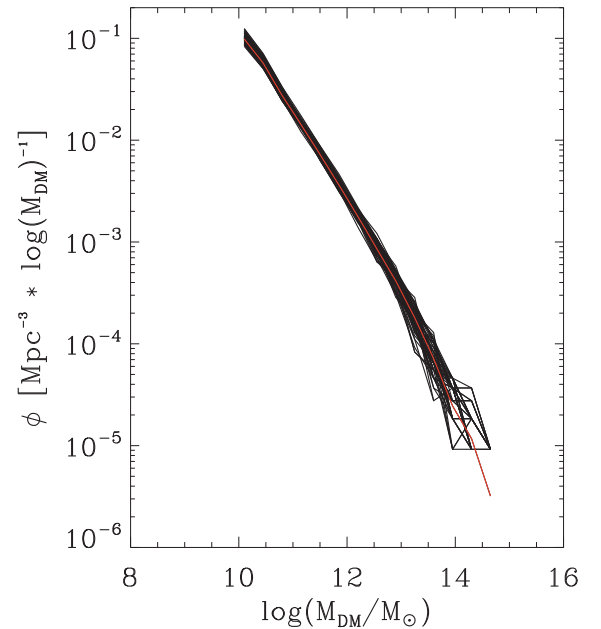
Figure 12. The FOF-mass function of dark matter haloes in a cosmological N-body simulation (red line) of volume $(100 \, \text{Mpc} \, h^{-1})^3$, and in 50 spherical sub-volumes of the size of the ATLAS[3D] volume, placed randomly within the large simulation. The effect of cosmic variance is clearly visible at the massive end of the mass function.

The fraction of fast rotators in Fig. 13 shows fluctuations at $M_K \gtrsim -25$, which are well within the error bars of the observed sample. Only for more luminous galaxies the fraction of fast rotators is heavily affected by cosmic variance. However, the fraction of fast rotators in the highest luminosity bin is on average still below
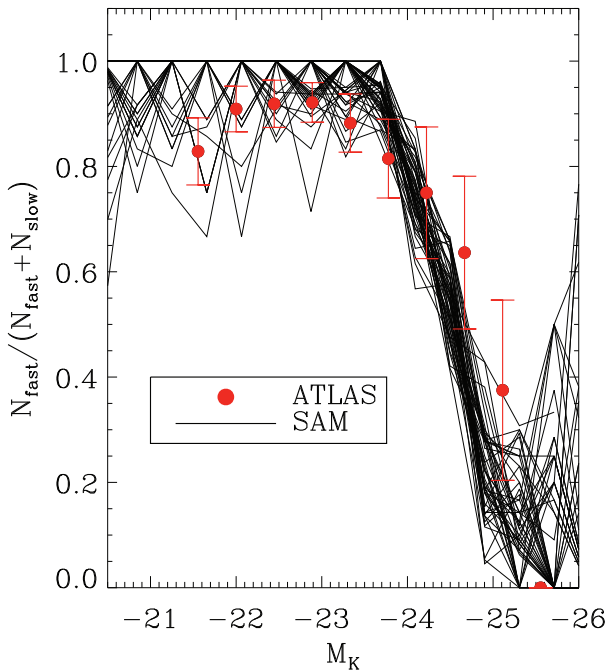
Figure 13. Same as Fig. 5 for 50 random spherical sub-volumes within a large-scale cosmological *N*-body simulation. The cosmological simulation itself has a volume of $(100 \, \text{Mpc} \, h^{-1})^3$ and each sub-volume has a volume comparable to that covered by the ATLAS^{3D} sample, i.e. $V_{A3D} = 10^5 \, \text{Mpc}^3$. Our results show that cosmic variance should not play a large role for the ATLAS^{3D} sample at $M_K > -25$. Only the fraction of fast rotators at the very luminous end might be affected by cosmic variance.

30 per cent. In terms of the ATLAS^{3D} sample our results suggest that the general trend of a declining fraction of fast rotators as a function of luminosity is robust and not affected by cosmic variance.

7.0.2 *Variations in merger histories*

Besides changes to the dark matter mass function in a given volume the individual merging history of the dark matter haloes might be different as well, and have a significant impact on the population of ETGs. We investigate the impact of the merger histories by generating 30 random merging histories for the dark matter mass function drawn from one of the sub-volumes. Again, we apply our fiducial model to predict the fraction of fast and slow rotators. The scatter about the median value is well within the error bars of the observations (Fig. 14), and large deviations only occur at $M_K \lesssim -25$. The magnitude of the scatter is comparable to the one seen for different mass functions and suggests that part of it might be initially due to the varying merger histories and only to the second order by the different number densities of haloes in a given volume. Varying merging histories has most impact at the extreme high-mass tail, where the relatively small number of major mergers can be strongly influenced by a few more major mergers during the history of a galaxy.

8 DISCUSSION AND SUMMARY

In this study, we have used an SAM approach that by construction reproduces first order key observations, such as the mass function, the trend in B/T as a function of stellar mass and the gas fraction in late-type galaxies. On top of this model we have made a selection of ETGs that tries to be as close to the ATLAS^{3D} (Paper I) selection
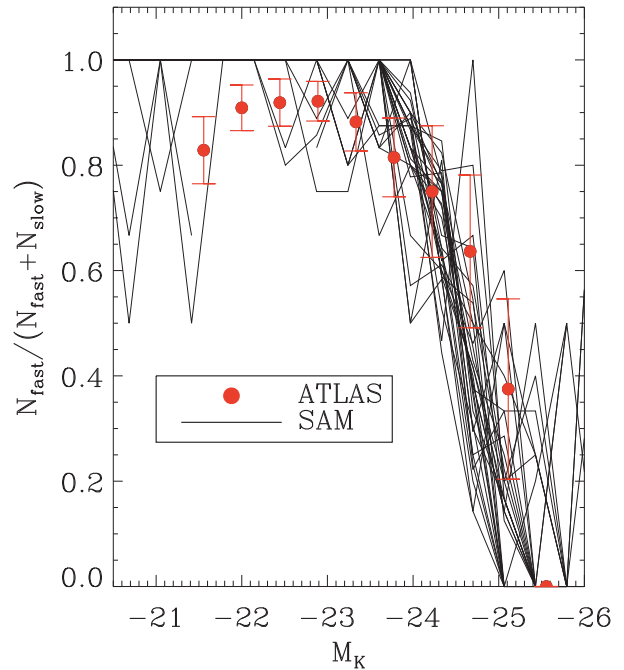
Figure 14. Same as Fig. 13 but for 30 random merging trees using the same mass function of haloes at $z = 0$. Below $M_K \sim -25$ results are robust and within the errors. The fraction of fast rotators at very low and very high luminosity is heavily affected by the individual merging histories of dark matter haloes.

as possible. While historically *B/T* (K99; Simien & de Vaucouleurs 1986) has been the preferred choice, in this study we extended this criterion to take into account the revised definition of ETGs proposed by the ATLAS^{3D} survey (Paper I). We introduce the additional condition of low cold gas fractions in disc-dominated galaxies to account for the population of flattened gas-poor fast-rotating ETGs in the ATLAS^{3D} sample. Support for this approach comes from the observed distribution of gas fractions in late-type galaxies and ETGs in the ATLAS^{3D} parent sample (Sarra et al., in preparation), and from the fact that binary mergers in general do not result in fast rotators as flat as observed (Paper VI). Anyway, the fraction of model fast rotators with low *B/T* and low gas fractions is only 22 per cent and is mainly affecting the low-mass end, where fast rotators dominate in any case. We thus expect this ETG selection not to change any trend seen between the fraction of fast and slow rotators at high masses. Based on these ETG selection criteria our model predicts a number density of ETGs in good agreement with the ATLAS^{3D} parent sample. We did not apply any 'fine-tuning' to match the number densities of ETGs, and these are just the outcome of the selection procedure that we applied. It is interesting to note that more than 80 per cent of ETGs in our sample have *B/T* values consistent with the classical selection of E and S0 galaxies based on the Hubble T-type and bulge-to-total light ratios (Simien & de Vaucouleurs 1986). Similar agreement has been found between the T-type based morphological definition and the ATLAS^{3D} ETG selection (Paper I) further supporting that our model ETG selection is close to the ATLAS^{3D} one.

In our model we grow bulges only via mergers and we neglect internal processes like disc instabilities that have been suggested as additional ways to grow bulges (e.g. Parry, Eke & Frenk 2009; Dekel, Sari & Ceverino 2009b). These processes are most efficient in gas-rich massive discs and would result in an increased fraction

of fast rotators with respect to our fiducial model with a range in B/T ratios depending on when the disc becomes stable. In such models clumps form in the disc and migrate due to dynamical friction into a central bulge. It is, however, not clear at this point whether such clumps survive long enough to reach the centre or get disrupted by feedback from supernovae (Genel et al. 2010).

Another important ingredient in our model is the ability to cool gas and re-grow discs. While SAMs in general reproduce the average cooling behaviour of gas in smoothed particle hydrodynamics (SPH) simulations there are differences when comparing on an object-to-object basis (Saro et al. 2010). Even between individual SAMs deviations in the calculated cooling rates exist (De Lucia et al. 2010). In general, the fraction of massive slow rotators is not affected by changes in the cooling rate, due to the constraint that the galaxy mass function needs to be reproduced. This is usually achieved by feedback implementations in the SAMs, which regulate the cooling of gas and the overall star formation. SPH simulations show that feedback plays indeed a key role in regulating gas accretion rates and star formation (e.g. van de Voort et al. 2010; Schaye et al. 2010). In our model we 'tune' our feedback efficiency and hence our cooling rate in such a way that we reproduce by construction the following observables: the stellar mass function, the gas fraction in late-type galaxies and the cooling rate in galaxies at high z. Using this approach we try to minimize the freedom in our cooling rates.

Besides cooling of gas, mass loss from already existing stars can provide significant material for the growth of stellar discs (Martig & Bournaud 2010; Agertz, Teyssier & Moore 2011; Kimm, Yi & Khochfar 2011). We do not take this into account in our model, but note here that such mass loss is likely to decrease the B/T of galaxies. Martig & Bournaud (2010) find that the Hubble T-type of a galaxy can change via this process by two to three units, affecting the fraction of fast rotators.

The merger rate of galaxies is a key aspect in our modelling approach. Being able to reproduce the stellar mass function, we populate dark matter haloes on average with galaxies of the right mass. Thus, when dark matter haloes merge we expect to merge the 'right' galaxies as well. In fact, the derived merger rates and average number of mergers from our model are in very good agreement with observations (Jogee et al. 2009; Conselice & Arnold 2009).

Within the ETGs selection we distinguish between fast and slow rotators based on the fraction of stellar disc still present in the main body. The main reasoning behind this approach is the observational fact that many fast rotators show regular rotation patterns and signs of bars (Paper II), which indicate the presence of a disc-like component (Paper VII). In addition, disc galaxies show values of $\lambda_R > 0.5$ similar to fast-rotating ETGs in the ATLAS^{3D} sample (Paper VI). In Paper VI the results of binary mergers have been extensively compared to the structure of galaxies in the ATLAS^{3D} sample showing that binary disc mergers reproduce best the properties of fast rotators with $\lambda_R \sim 0.25$–0.5, while fast rotators with $\lambda_R < 0.25$ are mostly reproduced in re-mergers of disc merger remnants, and that the majority of slow rotators cannot have formed from a binary major merger or re-merger. They in general have a much more complex formation history that will be investigated in Naab et al. (in preparation) and Bois et al. (in preparation). Paper VI shows that major mergers efficiently reduce λ_R in the central regions. Minor mergers on the contrary are expected to reduce λ_R in the outer regions. These results suggest that within the fast rotator population a sequence of mergers will preferentially lead to a reduction of λ_R. The way this can be naturally achieved is by the destruction of progenitor disc components via violent relax-

ation during mergers. However, discs can re-build by gas accretion and star formation increasing λ_R, and it is therefore important to model the complete merging history of a present-day ETG to decide on its status in terms of fast or slow rotation. We here do not attempt to model the detailed structures of fast- and slow-rotating ETGs but try to give answers on the average formation path of these galaxies. To achieve this we introduce a free model parameter, the minimum disc fraction required in fast rotators to divide our model ETG sample into fast and slow rotators. This parameter has been set to $f_{fast} = 0.1$ by matching the fraction of fast and slow rotators as a function of magnitude and their number density at $z = 0$, and serves the dual purpose of a free model parameter as well as a prediction of the expected disc fraction in fast rotators that can be compared to observations, once proper bulge–disc decompositions of ATLAS^{3D} galaxies have been performed. Effectively our model assumes that λ_R is to the first order a proxy for the disc fraction in ETGs.

The modelled fast and slow rotators show clear distinct growth histories, supporting the observationally motivated separation into two classes. The two main differences are that slow rotators grow by more accretion of stellar mass from satellites than fast rotators of the same mass, and that they have on average more major mergers.

The fraction of accreted material depends strongly on the competing effects of disc growth in galaxies and their destruction during mergers. While fast rotators continue accreting small levels of gas and forming stars in their recent history, consistent with observed star formation in ETGs (Schawinski et al. 2009), slow rotators completely stop accreting gas, and only grow via mergers. The main mechanism causing cooling to stop in high-mass galaxies is still debated and could have several different origins (see e.g. Croton et al. 2006; Cattaneo et al. 2006; Khochfar & Ostriker 2008; Johansson et al. 2009). We here adopt an empirical sharp transition in the cooling behaviour of gas based on a critical dark halo mass. It is likely that such a transition should in reality be smooth based on the underlying physics. Introducing a scatter in the critical halo mass, to model a smooth transition, is not changing the general growth properties of fast and slow rotators though. It is therefore safe to assume that whatever physical process causes cooling to stop in massive haloes, as long as it scales with galaxy mass, respectively halo mass, it will not change the growth history of fast and slow rotators. Completely neglecting any cooling shut-off results in too many massive galaxies (Croton et al. 2006), and in particular too many massive fast rotators.

The higher accretion fraction in slow rotators has another direct implication for the hot halo gas. The potential energy of infalling satellite galaxies is an effective source of gravitational heating of the hot halo gas (Khochfar & Ostriker 2008; Johansson et al. 2009). Either via dynamical friction heating (El-Zant, Kim & Kamionkowski 2004) or shocks large parts of the potential energy transfer to the halo gas. Our model thus naturally predicts to find preferentially hot X-ray haloes around slow rotators, and not fast rotators of the same mass (Sarzi et al. 2010), suggesting that X-ray haloes are a consequence of the mass assembly of an ETG.

Another important consequence of the higher accretion fractions in slow rotators is that even though they have the same average number of minor mergers as fast rotators of the same mass, the masses of the satellites are higher and the relative contribution towards lowering λ_R is much more important. Higher accretion fraction means higher disc destruction fraction through violent relaxation during the evolution of a galaxy, and thus lower λ_R. We find on average less than 10 minor mergers for the most massive progenitors of fast and slow rotators (Fig. 11), which allows the mass

distribution of merging satellites to be different for fast and slow rotators.

The average cold gas fraction of satellite galaxies merging with progenitors of present-day slow rotators is lower than that of fast rotators. This bias is a direct consequence of the fact that the infalling galaxies in slow rotators are more massive and thus have lower gas fractions (see Fig. 4), which hinders additionally the rebuilding of discs.

The second main difference in the growth history of fast and slow rotators is the number of major mergers. Slow rotators have on average more than twice as many major mergers than fast rotators. However, even the most massive ones do not have more than three major mergers on average during their evolution. We find that most of these major mergers happen at early times between gas-rich progenitors comparable to those simulated in Paper VI and Wuyts et al. (2010). Such gas-rich major mergers produce KDC similar to ones observed in present-day slow rotators (Paper VI). However, the remnants from major merger simulations tend to be not round enough compared to observations. Based on the merging history in our SAM we find that many minor mergers follow such a major merger event. Minor mergers from random directions (Khochfar & Burkert 2006), if not too compact, get stripped of their stellar material in the outer parts of the host galaxy, providing an envelope of stars that can make too flat major merger remnants with KDCs become more round. Further indirect evidence for the importance of minor mergers for the growth of a host galaxy particularly in its outer layers comes from the observed size evolution of ETGs (e.g. Khochfar & Silk 2006b; Trujillo et al. 2007; Bezanson et al. 2009; Naab et al. 2009; Hopkins et al. 2010c). As shown in Paper VI KDCs are very fragile during major mergers. Their observed presence in slow rotators prompts the question how they can survive till today. Analysing the growth history of slow rotators in our model, we find that in most of the cases the last gas-rich major merger was not very recent ($z > 1.5$) [see however Duc et al. (2011) for the case of a remnant from a possible recent gas-rich major merger], and that the number of major mergers is just not very high (see Fig. 10), both favouring the survival of KDCs in slow rotators. In contrast, fast rotators have on average less than one major merger in their history, making them unlikely candidates to host large-scale KDCs.

Within our model we predict a strong evolution of the slow rotator fraction towards low z. At $z \sim 2$ the number density of massive ($M_* > 10^{10}\,M_\odot$) fast rotators is more than one order of magnitude larger than the slow rotators one. This is mainly due to high cooling rates and gas fractions in mergers promoting stellar disc building over destruction. The evolution towards low redshifts is driven by the inability to efficiently re-build stellar disc in massive host galaxies, which is another representation of down sizing in star formation.

9 CONCLUSIONS

In this paper we made use of the completeness of the ATLAS^{3D} sample to investigate the origin and formation history of fast and slow rotator ETGs within a self-consistent cosmological framework using the semi-analytical modelling approach. We here present a model in which the difference between fast and slow rotator ETGs is purely based on the stellar disc fraction found in them, and predict that fast rotators have disc fractions $M_{\rm disc}/M_* > 0.1$. We find that slow rotators within an evolving universe mark the transition in the ability of galaxies to cool gas and to rebuild stellar discs. We find a clear separation in the growth history of fast and slow rotator ETGs, supporting the observationally motivated distinction. In particular,

the accreted fraction of stars shows a clear distinction between fast and slow rotators, with the latter having between 50 and 90 per cent of their stellar mass accreted from satellites while the former has <50 per cent accreted.

Although we find a clear separation into fast and slow rotators, we also find that ETGs can switch their state between fast and slow rotator and vice versa based on stellar disc growth or destruction by mergers, suggesting that fast and slow rotator ETGs are transient. These changes, however, occur predominantly at higher redshifts when cooling is more efficient and mergers more frequent. The fraction of slow rotators shows a continued increases with time due to the conversion of fast rotators and the inability of gas to cool and convert slow rotators back to fast rotators. Massive present-day slow rotators therefore can be viewed as the final stage in the evolution of ETGs.

Future high-redshift observations of ETGs will be able to reveal any possible evolution in the fraction of fast and slow rotators and test the presented model further.

REFERENCES

Agertz O., Teyssier R., Moore B., 2011, MNRAS, 410, 1391

Almeida C., Baugh C. M., Lacey C. G., 2007, MNRAS, 376, 1711

Barnes J. E., Hernquist L. E., 1991, ApJ, 370, L65

Barnes J. E., Hernquist L., 1992, ARA&A, 30, 705

Bell E. F., de Jong R. S., 2001, ApJ, 550, 212

Bell E. F., McIntosh D. H., Katz N., Weinberg M. D., 2003, ApJS, 149, 289

Bender R., Surma P., Doebereiner S., Moellenhoff C., Madejsky R., 1989, A&A, 217, 35

Bendo G. J., Barnes J. E., 2000, MNRAS, 316, 315

Benson A. J., Bower R. G., Frenk C. S., Lacey C. G., Baugh C. M., Cole S., 2003, ApJ, 599, 38

Bernardi M. et al., 2003, AJ, 125, 1817

Bett P., Eke V., Frenk C. S., Jenkins A., Helly J., Navarro J., 2007, MNRAS, 376, 215

Bezanson R., van Dokkum P. G., Tal T., Marchesini D., Kriek M., Franx M., Coppi P., 2009, ApJ, 697, 1290

Binney J., 1978, MNRAS, 183, 501

Birnboim Y., Dekel A., 2003, MNRAS, 345, 349

Bois M. et al., 2010, MNRAS, 406, 2405

Bois M. et al., 2011, MNRAS, 416, 1654 (Paper VI)

Bournaud F., Combes F., Jog C. J., 2004, A&A, 418, L27

Bournaud F., Jog C. J., Combes F., 2007, A&A, 476, 1179

Bower R. G., Benson A. J., Malbon R., Helly J. C., Frenk C. S., Baugh C. M., Cole S., Lacey C. G., 2006, MNRAS, 370, 645

Bruzual G., Charlot S., 2003, MNRAS, 344, 1000

Cappellari M. et al., 2007, MNRAS, 379, 418

Cappellari M. et al., 2011a, MNRAS, 413, 813 (Paper I)

Cappellari M. et al., 2011b, MNRAS, 416, 1680 (Paper VII)

Cattaneo A., Dekel A., Devriendt J., Guiderdoni B., Blaizot J., 2006, MNRAS, 370, 1651

Cole S., Lacey C. G., Baugh C. M., Frenk C. S., 2000, MNRAS, 319, 168

Combes F., 2009, in Jogee S., Marinova I., Hao L., Blanc G. A., eds, ASP Conf. Ser. Vol. 419, Galaxy Evolution: Emerging Insights and Future Challenges. Astron. Soc. Pac., San Francisco, p. 31

Conselice C. J., Arnold J., 2009, MNRAS, 397, 208

Conselice C. J., Bershady M. A., Dickinson M., Papovich C., 2003, AJ, 126, 1183

Cox T. J., Dutta S. N., Di Matteo T., Hernquist L., Hopkins P. F., Robertson B., Springel V., 2006, ApJ, 650, 791

Croton D. J. et al., 2006, MNRAS, 365, 11

Crockett R. M. et al., 2011, ApJ, 727, 115

Davies R. L., Efstathiou G., Fall S. M., Illingworth G., Schechter P. L., 1983, ApJ, 266, 41

De Lucia G., Blaizot J., 2007, MNRAS, 375, 2

De Lucia G., Springel V., White S. D. M., Croton D., Kauffmann G., 2006, MNRAS, 366, 499

De Lucia G., Boylan-Kolchin M., Benson A. J., Fontanot F., Monaco P., 2010, MNRAS, 406, 1533

de Zeeuw P. T. et al., 2002, MNRAS, 329, 513

Dekel A., Birnboim Y., 2008, MNRAS, 383, 119

Dekel A., Silk J., 1986, ApJ, 303, 39

Dekel A. et al., 2009a, Nat, 457, 451

Dekel A., Sari R., Ceverino D., 2009b, ApJ, 703, 785

Dressler A., 1980, ApJ, 236, 351

Duc P.-A. et al., 2011, MNRAS, in press (doi:10.1111/j.1365-2966.2011.19137.x) (Paper IX, this issue)

El-Zant A. A., Kim W.-T., Kamionkowski M., 2004, MNRAS, 354, 169

Emsellem E. et al., 2007, MNRAS, 379, 401

Emsellem E. et al., 2011, MNRAS, 687 (Paper III)

Ferrarese L., van den Bosch F. C., Ford H. C., Jaffe W., O'Connell R. W., 1994, AJ, 108, 1598

Ferreras I., Lisker T., Pasquali A., Khochfar S., Kaviraj S., 2009, MNRAS, 396, 1573

Genel S. et al., 2010, preprint (arXiv:1011.0433)

Gnedin N. Y., 2000, ApJ, 542, 535

Granato G. L., De Zotti G., Silva L., Bressan A., Danese L., 2004, ApJ, 600, 580

Hatton S., Devriendt J. E. G., Ninin S., Bouchet F. R., Guiderdoni B., Vibert D., 2003, MNRAS, 343, 75

Hoffman L., Cox T. J., Dutta S., Hernquist L., 2010, ApJ, 723, 818

Hopkins P. F., Hernquist L., Cox T. J., Dutta S. N., Rothberg B., 2008, ApJ, 679, 156

Hopkins P. F., Cox T. J., Younger J. D., Hernquist L., 2009a, ApJ, 691, 1168

Hopkins P. F. et al., 2009b, MNRAS, 397, 802

Hopkins P. F., Lauer T. R., Cox T. J., Hernquist L., Kormendy J., 2009c, ApJS, 181, 486

Hopkins P. F. et al., 2010a, ApJ, 715, 202

Hopkins P. F. et al., 2010b, ApJ, 724, 915

Hopkins P. F., Bundy K., Hernquist L., Wuyts S., Cox T. J., 2010c, MNRAS, 401, 1099

Jenkins A., Frenk C. S., White S. D. M., Colberg J. M., Cole S., Evrard A. E., Couchman H. M. P., Yoshida N., 2001, MNRAS, 321, 372

Jesseit R., Naab T., Burkert A., 2005, MNRAS, 360, 1185

Jesseit R., Cappellari M., Naab T., Emsellem E., Burkert A., 2009, MNRAS, 397, 1202

Jiang C. Y., Jing Y. P., Faltenbacher A., Lin W. P., Li C., 2008, ApJ, 675, 1095

Jogee S. et al., 2009, ApJ, 697, 1971

Johansson P. H., Naab T., Ostriker J. P., 2009, ApJ, 697, L38

Kang X., Jing Y. P., Silk J., 2006, ApJ, 648, 820

Kang X., van den Bosch F. C., 2008, ApJ, 676, L101

Kannappan S. J., 2004, ApJ, 611, L89

Kauffmann G., Colberg J. M., Diaferio A., White S. D. M., 1999, MNRAS, 303, 188 (K99)

Kaviraj S., Peirani S., Khochfar S., Silk J., Kay S., 2009, MNRAS, 394, 1713

Kaviraj S., Tan K.-M., Ellis R. S., Silk J., 2011, MNRAS, 411, 2148

Kennicutt R. C., Jr, 1998, ApJ, 498, 541

Kereš D., Katz N., Weinberg D. H., Davé R., 2005, MNRAS, 363, 2

Kereš D., Katz N., Fardal M., Davé R., Weinberg D. H., 2009, MNRAS, 395, 160

Khochfar S., Burkert A., 2001, ApJ, 561, 517

Khochfar S., Burkert A., 2003, ApJ, 597, L117

Khochfar S., Burkert A., 2005, MNRAS, 359, 1379

Khochfar S., Burkert A., 2006, A&A, 445, 403

Khochfar S., Ostriker J. P., 2008, ApJ, 680, 54

Khochfar S., Silk J., 2006a, MNRAS, 370, 902

Khochfar S., Silk J., 2006b, ApJ, 648, L21

Khochfar S., Silk J., 2009a, MNRAS, 397, 506

Khochfar S., Silk J., 2009b, ApJ, 700, L21

Khochfar S., Silk J., Windhorst R. A., Ryan R. E., Jr, 2007, ApJ, 668, L115

Kimm T., Yi S. K., Khochfar S., 2011, ApJ, 729, 11

Komatsu E. et al., 2011, ApJS, 192, 18

Kormendy J., Bender R., 1996, ApJ, 464, L119

Kormendy J., Fisher D. B., Cornell M. E., Bender R., 2009, ApJS, 182, 216

Krajnović D. et al., 2008, MNRAS, 390, 93

Krajnović D. et al., 2011, MNRAS, 414, 2923 (Paper II)

Lacey C., Cole S., 1993, MNRAS, 262, 627

Larson R. B., 1974, MNRAS, 166, 585

Lauer T. R. et al., 1995, AJ, 110, 2622

Lynden Bell D., 1967, MNRAS, 136, 101

McGaugh S. S., 2005, ApJ, 632, 859

Maller A. H., Dekel A., Somerville R., 2002, MNRAS, 329, 423

Martig M., Bournaud F., 2010, ApJ, 714, L275

Mihos J. C., Hernquist L., 1996, ApJ, 464, 641

Milosavljević M., Merritt D., 2001, ApJ, 563, 34

Mo H. J., Mao S., White S. D. M., 1998, MNRAS, 295, 319

Mulchaey J. S., Jeltema T. E., 2010, ApJ, 715, L1

Naab T., Burkert A., 2003, ApJ, 597, 893

Naab T., Trujillo I., 2006, MNRAS, 369, 625

Naab T., Khochfar S., Burkert A., 2006, ApJ, 636, L81

Naab T., Johansson P. H., Ostriker J. P., 2009, ApJ, 699, L178

Nagashima M., Lacey C. G., Okamoto T., Baugh C. M., Frenk C. S., Cole S., 2005, MNRAS, 363, L31

Negroponte J., White S. D. M., 1983, MNRAS, 205, 1009

Neistein E., Weinmann S. M., 2010, MNRAS, 405, 2717

Obreschkow D., Croton D., De Lucia G., Khochfar S., Rawlings S., 2009, ApJ, 698, 1467

Ocvirk P., Pichon C., Teyssier R., 2008, MNRAS, 390, 1326

Oser L., Ostriker J. P., Naab T., Johansson P. H., Burkert A., 2010, ApJ, 725, 2315

Parry O. H., Eke V. R., Frenk C. S., 2009, MNRAS, 396, 1972

Peirani S., Crockett R. M., Geen S., Khochfar S., Kaviraj S., Silk J., 2010, MNRAS, 405, 2327

Rees M. J., Ostriker J. P., 1977, MNRAS, 179, 541

Rix H.-W., White S. D. M., 1990, ApJ, 362, 52

Robertson B., Bullock J. S., Cox T. J., Di Matteo T., Hernquist L., Springel V., Yoshida N., 2006, ApJ, 645, 986

Sandage A., 1961, The Hubble Atlas. Carnegie Institution, Washington

Saro A., De Lucia G., Borgani S., Dolag K., 2010, MNRAS, 406, 729

Sarzi M. et al., 2010, MNRAS, 402, 2187

Schawinski K. et al., 2009, MNRAS, 396, 818

Schaye J. et al., 2010, MNRAS, 402, 1536

Shankar F., Marulli F., Bernardi M., Boylan-Kolchin M., Dai X., Khochfar S., 2010, MNRAS, 405, 948

Silk J., 1977, ApJ, 211, 638

Simien F., de Vaucouleurs G., 1986, ApJ, 302, 564

Smith M. C. et al., 2007, MNRAS, 379, 755

Somerville R. S., 2002, ApJ, 572, L23

Somerville R. S., Kolatt T. S., 1999, MNRAS, 305, 1

Somerville R. S., Primack J. R., 1999, MNRAS, 310, 1087

Somerville R. S., Lemson G., Kolatt T. S., Dekel A., 2000, MNRAS, 316, 479

Springel V., 2005, MNRAS, 364, 1105

Springel V., White S. D. M., Tormen G., Kauffmann G., 2001, MNRAS, 328, 726 (S01)

Sutherland R. S., Dopita M. A., 1993, ApJS, 88, 253

Thomas D., Maraston C., Bender R., Mendes de Oliveira C., 2005, ApJ, 621, 673

Toomre A., Toomre J., 1972, ApJ, 178, 623

Trujillo I., Conselice C. J., Bundy K., Cooper M. C., Eisenhardt P., Ellis R. S., 2007, MNRAS, 382, 109

van de Voort F., Schaye J., Booth C. M., Haas M. R., Dalla Vecchia C., 2011, MNRAS, 414, 2458

van der Wel A., Bell E. F., van den Bosch F. C., Gallazzi A., Rix H.-W., 2009, ApJ, 698, 1232

Weinzirl T., Jogee S., Khochfar S., Burkert A., Kormendy J., 2009, ApJ, 696, 411

White S. D. M., 1978, MNRAS, 184, 185

White S. D. M., Frenk C. S., 1991, ApJ, 379, 52

White S. D. M., Rees M. J., 1978, MNRAS, 183, 341

Wuyts S., Cox T. J., Hayward C. C., Franx M., Hernquist L., Hopkins P. F., Jonsson P., van Dokkum P. G., 2010, ApJ, 722, 1666

Young L. M. et al., 2011, MNRAS, 414, 940 (Paper IV)

This paper has been typeset from a TEX/LATEX file prepared by the author.